Physics 224 - Spring 2010

Origin and Evolution of the Universe

Week 9
Cosmic Web

Joel Primack
University of California, Santa Cruz

Physics 224 - Spring 2010

Origin and Evolution of the Universe

Week	Topics
1	Historical Introduction
2	General Relativistic Cosmology
3	Big Bang Nucleosynthesis
4	Recombination, Dark Matter
5	Dark Matter, Topological Defects
6	Cosmic Inflation
7	Before and After Cosmic Inflation
8	Baryogenesis, CMB, Structure Formation
9	Cosmic Web
10	Galaxy Formation and Evolution
11	Student Presentations

The Linear Transfer Function T(k)

The observed uniformity of the CMB guarantees that density fluctuations must have been quite small at decoupling, implying that the evolution of the density contrast can be studied at $z \lesssim z_{\rm dec}$ using linear theory, and each mode $\delta(k)$ evolves independently. The inflationary model predicts a scale-inv$\approx$iant primordial power spectrum of density fluctuations $P(k) \equiv \langle|\delta(k)|^2\rangle \propto k^n$, with $n = 1$ (the so-called Harrison-Zel'dovich spectrum). It is the index n that governs the balance between large and small-scale power. In the case of a Gaussian random field with zero mean, the power spectrum contains the complete statistical information about the density inhomogeneity. It is often more convenient to use the dimensionless quantity $\Delta_k^2 \equiv [k^3 P(k)/2\pi^2]$, which is the power per logarithmic interval in wavenumber k. In the matter-dominated epoch, this quantity retains its initial primordial shape ($\Delta_k^2 \propto k^{n+3}$) only on very large scales. Small wavelength modes enter the horizon earlier on and their growth is suppressed more severely during the radiation-dominated epoch: on small scales the amplitude of Δ_k^2 is essentially suppressed by four powers of k (from k^{n+3} to k^{n-1}). If $n = 1$, then small scales will have nearly the same power except for a weak, logarithmic dependence. Departures from the initially scale-free form are described by the transfer function $T(k)$, defined such that $T(0) = 1$:

$$P(k,z) = Ak^n \left[\frac{D(z)}{D(0)}\right]^2 T^2(k),$$

where A is the normalization.

An approximate fitting function for T(k) in a ΛCDM universe is (Bardeen et al. 1986)

$$T_k = \frac{\ln(1+2.34q)}{2.34q}\left[1+3.89q+(16.1q)^2+(5.46q)^3+(6.71q)^4\right]^{-1/4},$$

where (Sugayama 1995)

$$q \equiv \frac{k/\mathrm{Mpc}^{-1}}{\Omega_m h^2 \exp(-\Omega_b - \Omega_b/\Omega_m)}.$$

For accurate work, for example for starting high-resolution N-body simulations, it is best to use instead of fitting functions the numerical output of highly accurate integration of the Boltzmann equations, for example from CMBFast, which is available at
http://lambda.gsfc.nasa.gov/toolbox/ which points to
http://lambda.gsfc.nasa.gov/toolbox/tb_cmbfast_ov.cfm

W e l c o m e to the CMBFAST Website!

This is the most extensively used code for computing cosmic microwave background anisotropy, polarization and matter power spectra. The code has been tested over a wide range of cosmological parameters. We are continuously testing and updating the code based on suggestions from the cosmological community. Do not hesitate to contact us if you have any questions or suggestions.

U. Seljak & M. Zaldarriaga

CMB Toolbox Overview

We provide links to a number of useful tools for CMB and Astronomy in general.

CMB Tools

- CMB Simulations - High-resolution, full-sky microwave temperature simulations including secondary anisotropies.

- Contributed Software is an archive at a LAMBDA partner site for tools built by members of the community.
- CMBFast - A tool that computes spectra for the cosmic background for a given set of CMB parameters. LAMBDA provides a web-based interface for this tool. Seljak and Zaldarriaga
- CAMB - Code for Anisotropies in the Microwave Background that computes spectra for a set of CMB parameters. LAMBDA provides a web-based interface for this tool. Lewis and Challinor
- CMBEASY - A C++ package, initially based on CMBFAST, now featuring a parameter likelihood package as well. Doran
- CMBview - A Mac OS X program for viewing HEALPix-format CMB data on an OpenGL-rendered sphere. Portsmouth
- COMBAT - A set of computational tools for CMB analysis. Borrill et al.
- CosmoMC - A Markov-Chain Monte-Carlo engine for exploring cosmological parameter space. Lewis and Bridle
- CosmoNet - Accelerated cosmological parameter estimation using Neural Networks.
- GLESP - Gauss-Legendre sky pixelization package. Doroshkevich, et al.
- GSM - Predicted all-sky maps at any frequency from 10 MHz to 100 GHz. de Oliveira-Costa.
- HEALPix - A spherical sky pixelization scheme. The Wilkinson Microwave Anisotropy Probe (WMAP) data skymap products are supplied in this form. Górski et al.
- IGLOO - A sky pixelization package. Crittenden and Turok
- MADCAP - Microwave Anisotropy Data Computational Analysis Package. Borrill et al.
- PICO - Integrates with CAMB and/or CosmoMC for cosmological parameter estimation using machine learning. Wandelt and Fendt
- RADPACK - Radical Compression Analysis Package. Knox
- RECFAST- Software to calculate the recombination history of the Universe. Seager, Sasselov, and Scott
- SkyViewer - A LAMBDA-developed OpenGL-based program to display HEALPix-based skymaps stored in FITS format files. Phillips
- SpiCE - Spatially Inhomogenous Correlation Estimator. Szapudi et al.
- WMAPViewer - A LAMBDA-developed web-based CMB map viewing tool using a technology similar to that found on maps.google.com. Phillips
- WOMBAT - Microwave foreground emission tools. Gawiser, Finkbeiner, Jaff et al.

Likelihood Software

- SDSS LRG DR7 Likelihood Software - A software package that computes likelihoods for Luminous Red Galaxies (LRG) data from the seventh release of the Sloan Digital Sky Survey (SDSS).
- WMAP Likelihood Software - A software library used by the WMAP team to compute Fisher and Master matrices and to compute the likelihoods of various models. This is the same software found on the WMAP products list; more information may be found here.

Other Tools

- WMAP Effective Frequency Calculator - A tool that calculates the effective frequencies of the five WMAP frequency bands.
- CFITSIO - A library of C and Fortran routines for reading and writing data in the FITS format.
- IDL Astro - The IDL Astronomy Users Library.
- Conversion Utilities - A small collection of astronomical conversion utilities.
- Calculators - A list of links to calculators.

This collection of tools can only be extended and improved with your input! Please feel free to send us suggestions and comments.

Scale-Invariant Spectrum (Harrison-Zel'dovich)

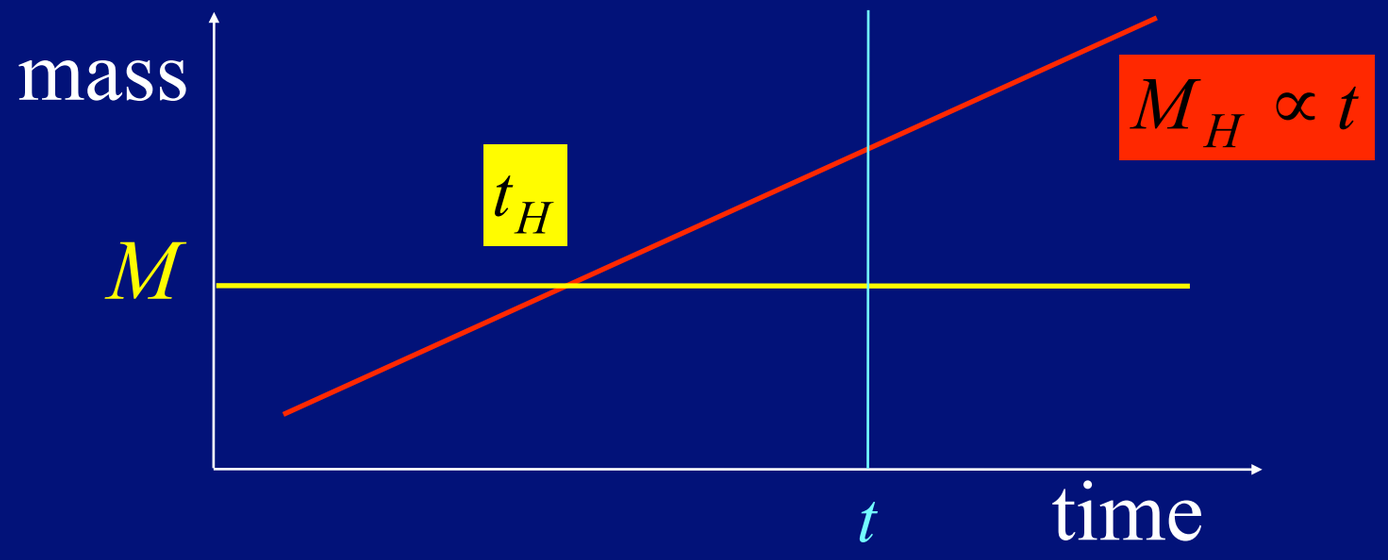

$$\delta(M,t) = \delta_H \left(\frac{t}{t_H(M)} \right)^{2/3} \propto M^{-2/3} t^{2/3}$$

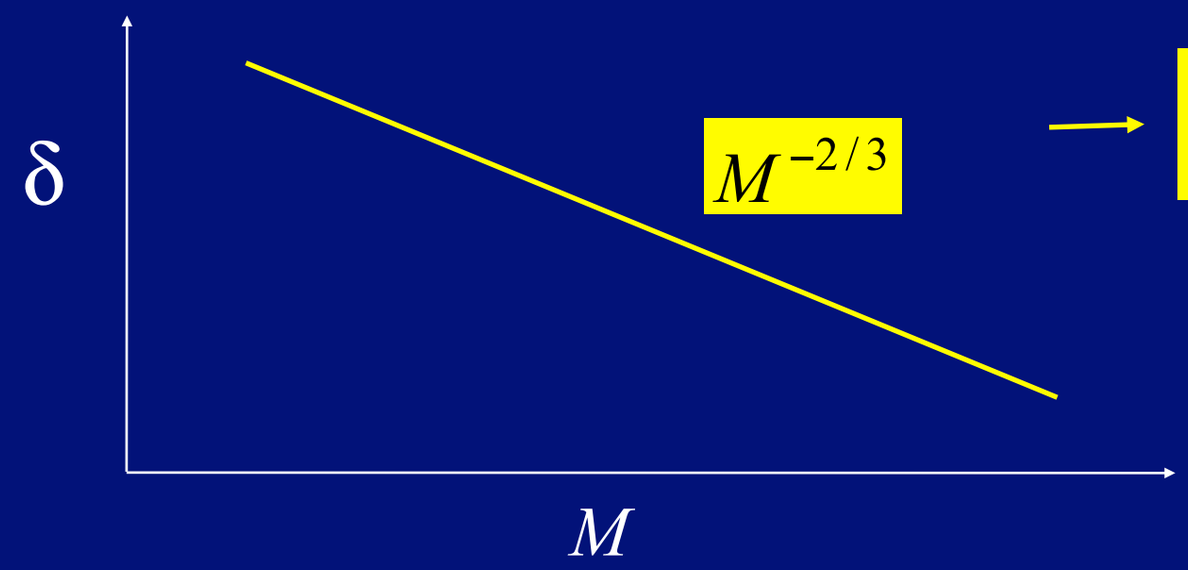

$$n = +1 \quad P_k \propto k$$

CDM Power Spectrum

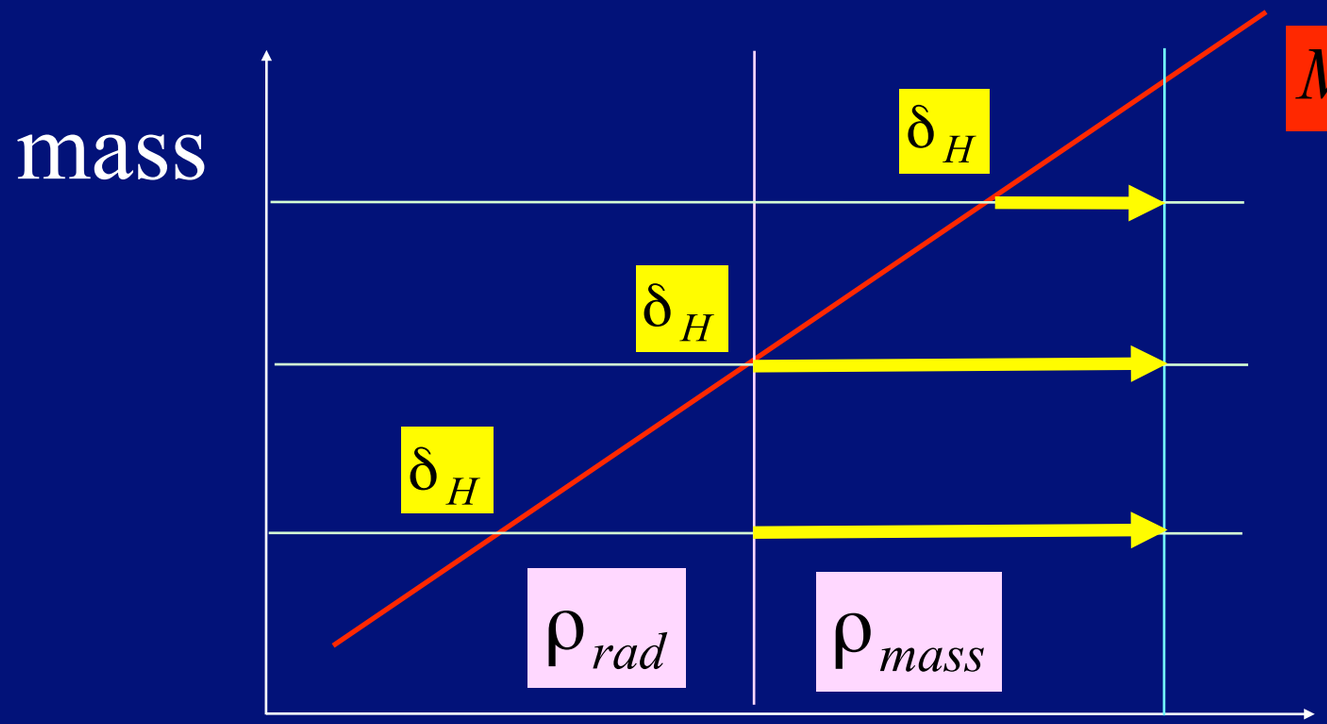

δ growth when matter is self-gravitating

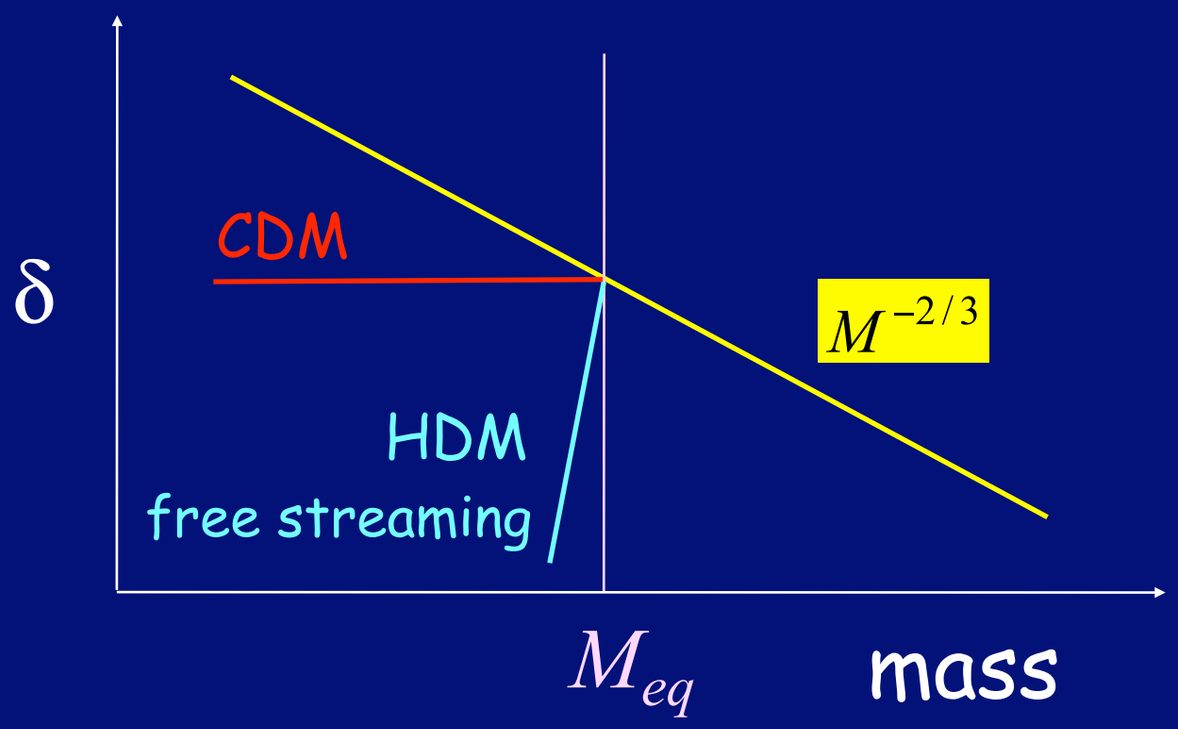

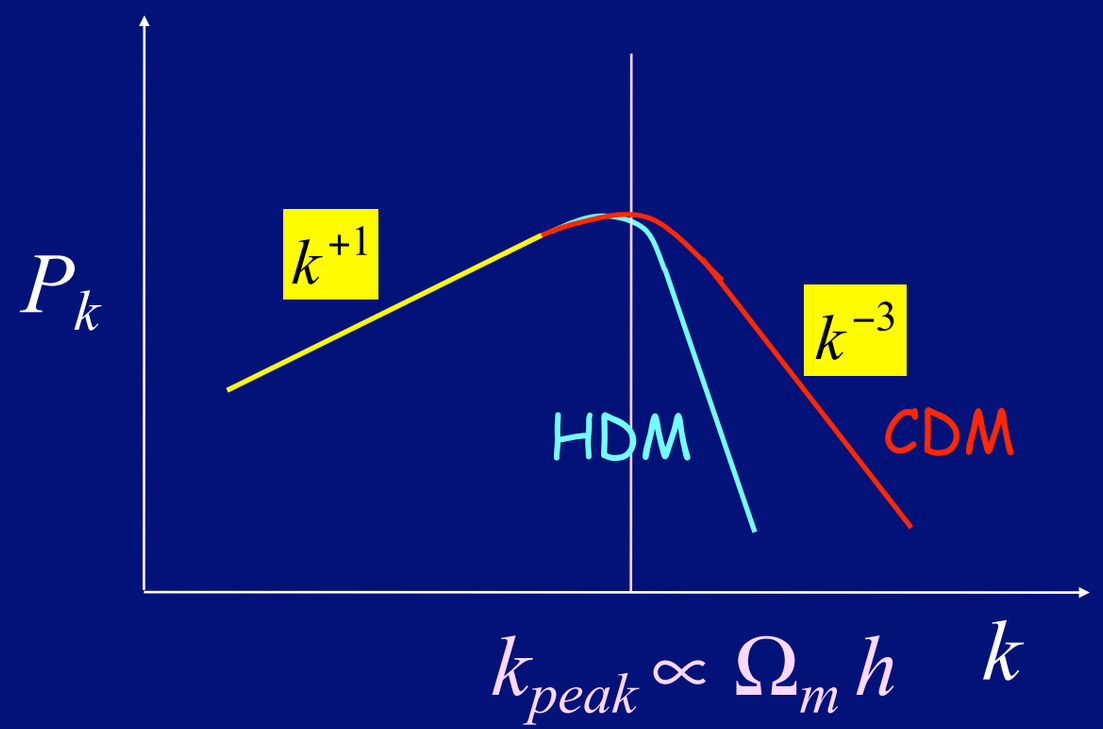

Formation of Large-Scale Structure

Fluctuation growth in the linear regime: $\delta << 1 \longrightarrow \delta \propto t^{2/3}$

rms fluctuation at mass scale M: $\delta \propto M^{-\alpha} \quad 0 < \alpha \leq 2/3$

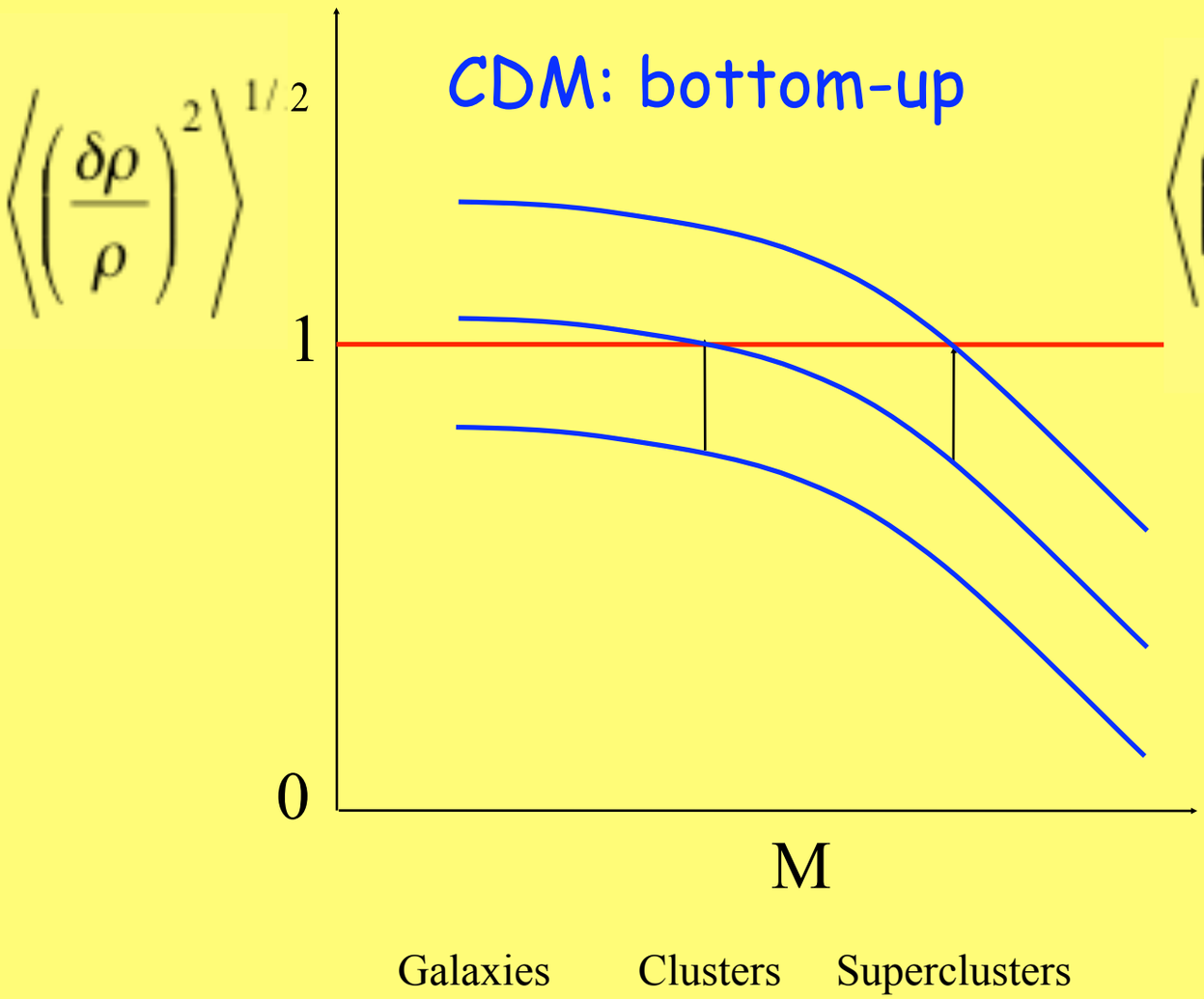

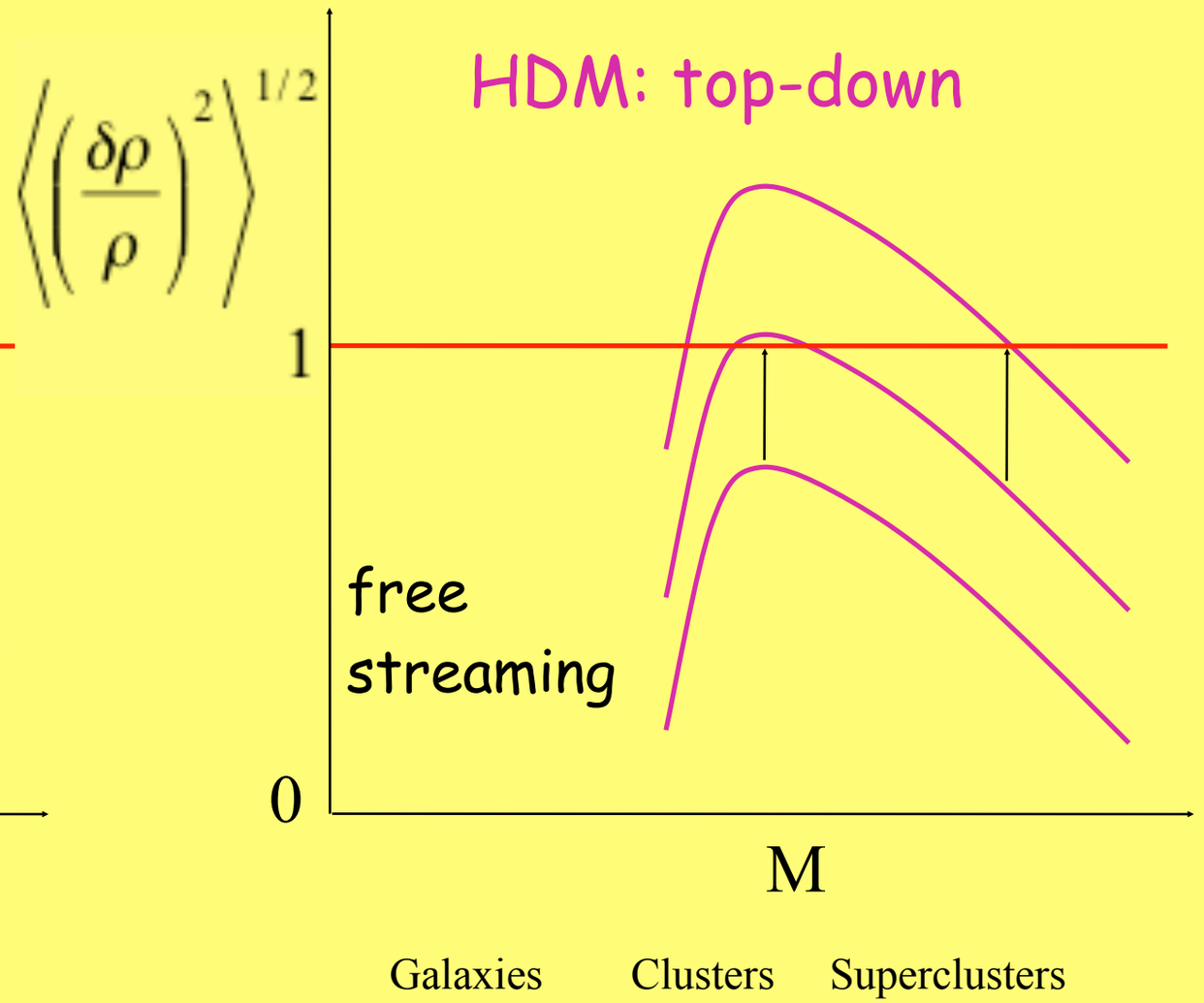

Structure forms earliest in Open, next in Benchmark, latest in EdS model.

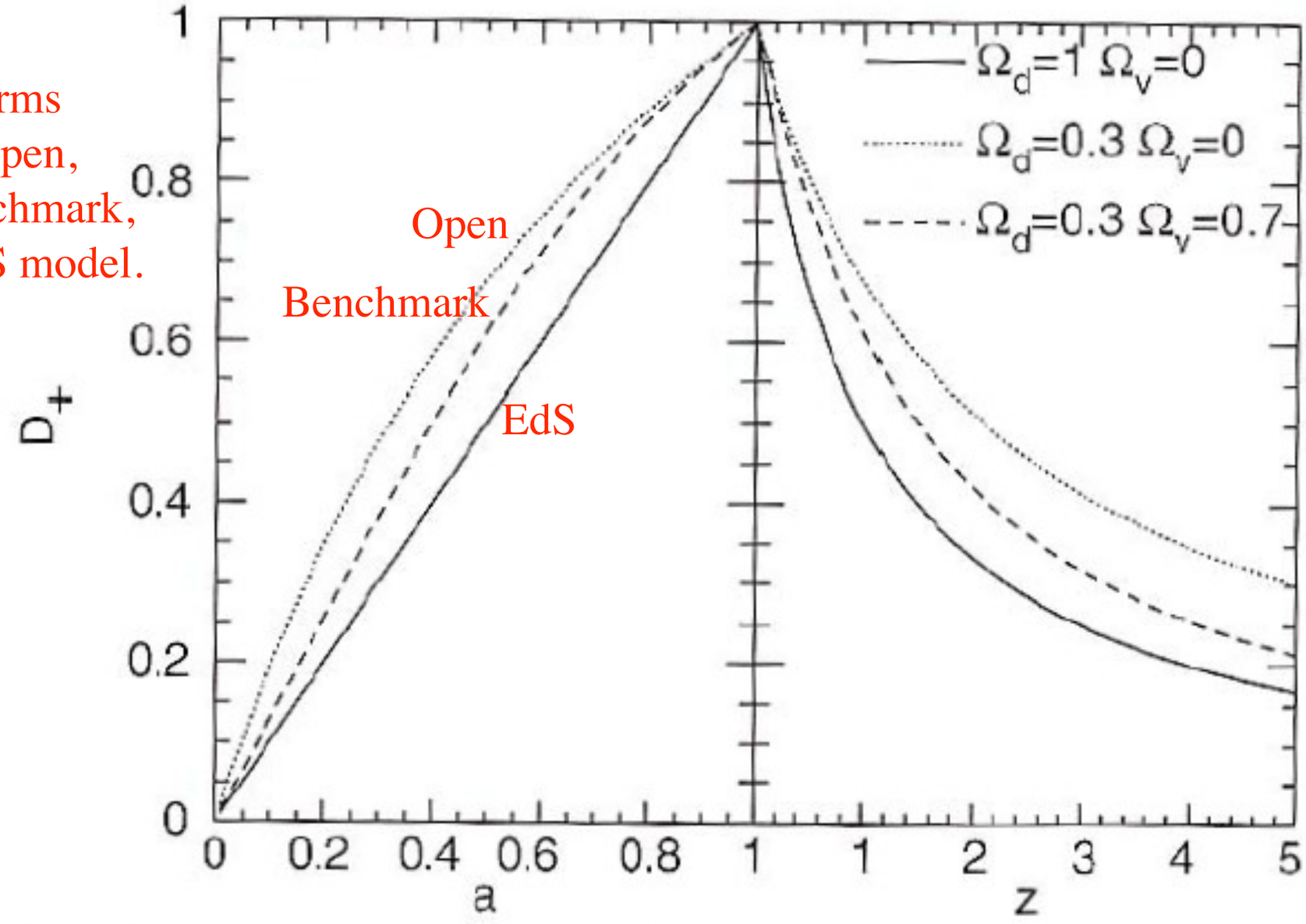

Einstein-de Sitter

Open universe

Benchmark model

Fig. 7.3. Growth factor D_+ for three different cosmological models, as a function of the scale factor a (left panel) and of redshift (right panel). It is clearly visible how quickly D_+ decreases with increasing redshift in the EdS model, in comparison to the models of lower density

From Peter Schneider, *Extragalactic Astronomy and Cosmology* (Springer, 2006)

Linear Growth Rate Function $D(a)$

For completeness, here we present some approximations used in the text. For the family of flat cosmologies ($\Omega_{\rm m}+\Omega_\Lambda=1$) an accurate approximation for the value of the virial overdensity $\Delta_{\rm vir}$ is given by the analytic formula (Bryan & Norman 1998):

$$\Delta_{\rm vir} = (18\pi^2 + 82x - 39x^2)/\Omega(z), \tag{A1}$$

where $\Omega(z) \equiv \rho_{\rm m}(z)/\rho_{\rm crit}$ and $x \equiv \Omega(z) - 1$.

The linear growth-rate function $\delta(a)$, used in eqs. (14-15) and also in $\sigma_8(a)$ is defined as

$$\delta(a) = D(a)/D(1), \tag{A2}$$

where $a = 1/(1+z)$ is the expansion parameter and $D(a)$ is:

$$D(a) = \frac{5}{2}\left(\frac{\Omega_{\rm m,0}}{\Omega_{\Lambda,0}}\right)^{1/3} \frac{\sqrt{1+x^3}}{x^{3/2}} \int_0^x \frac{x^{3/2}dx}{[1+x^3]^{3/2}}, \tag{A3}$$

$$x \equiv \left(\frac{\Omega_{\Lambda,0}}{\Omega_{\rm m,0}}\right)^{1/3} a, \tag{A4}$$

where $\Omega_{\rm m,0}$ and $\Omega_{\Lambda,0}$ are density contributions of matter and cosmological constant at $z=0$. For $\Omega_{\rm m} > 0.1$ the growth rate factor $D(a)$ can be accurately approximated by the following expressions (Lahav et al. 1991; Carroll et al. 1992):

$$D(a) = \frac{(5/2)a\Omega_{\rm m}}{\Omega_{\rm m}^{4/7} - \Omega_\Lambda + (1+\Omega_{\rm m}/2)(1+\Omega_\Lambda/70)}, \tag{A5}$$

$$\Omega_{\rm m}(a) = \Omega_{\rm m,0}/(1+x^3), \tag{A6}$$

$$\Omega_\Lambda(a) = 1 - \Omega_{\rm m}(a) \tag{A7}$$

For $\Omega_{\rm m,0} = 0.27$ the error of these approximation is less than 7×10^{-4}.

From Klypin, Trujillo, Primack - Bolshoi paper I - Appendix A

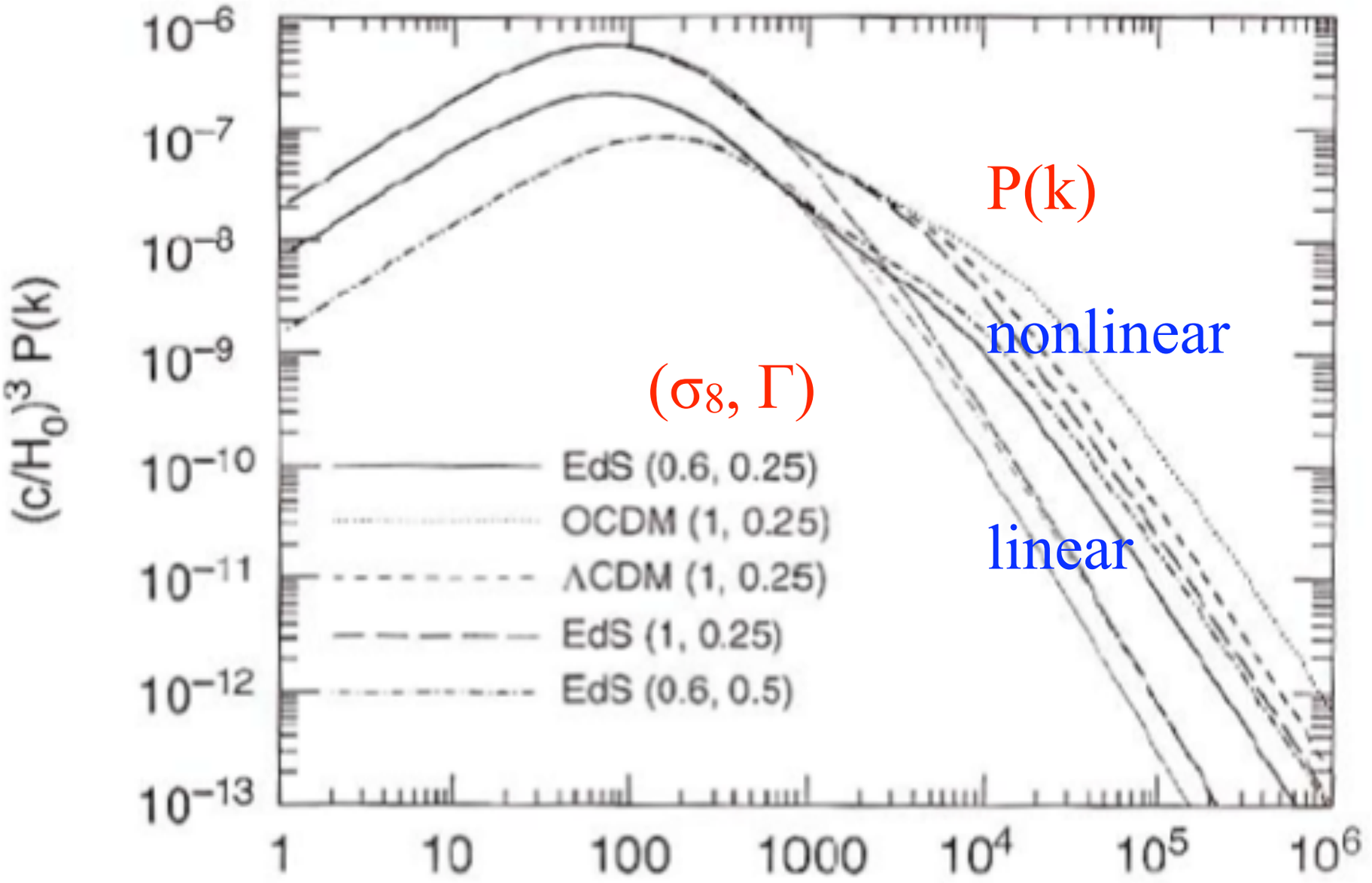

Fig. 7.6. The current power spectrum of density fluctuations for CDM models. The wave number k is given in units of H_0/c, and $(H_0/c)^3\ P(k)$ is dimensionless. The various curves have different cosmological parameters: EdS: $\Omega_m = 1$, $\Omega_\Lambda = 0$; OCDM: $\Omega_m = 0.3$, $\Omega_\Lambda = 0$; ΛCDM: $\Omega_m = 0.3$, $\Omega_\Lambda = 0.7$. The values in parentheses specify (σ_8, Γ), where σ_8 is the normalization of the power spectrum (which will be discussed below), and where Γ is the shape parameter. The thin curves correspond to the power spectrum $P_0(k)$ linearly extrapolated to the present day, and the bold curves take the non-linear evolution into account

From Peter Schneider, *Extragalactic Astronomy and Cosmology* (Springer, 2006)

On large scales (k small), the gravity of the dark matter dominates. But on small scales, pressure dominates and growth of baryonic fluctuations is prevented. Gravity and pressure are equal at the Jeans scale

$$k_J = \frac{a}{c_s}\sqrt{4\pi G\rho}.$$

The Jeans mass is the dark matter + baryon mass enclosed within a sphere of radius $\pi a/k_J$,

$$M_J = \frac{4\pi}{3}\rho\left(\frac{\pi a}{k_J}\right)^3 = \frac{4\pi}{3}\rho\left(\frac{5\pi k_B T_e}{12G\rho m_p \mu}\right)^{3/2} \approx 8.8\times 10^4\ \mathrm{M}_\odot \left(\frac{aT_e}{\mu}\right)^{3/2},$$

where μ is the mean molecular weight. The evolution of M_J is shown below, assuming that reionization occurs at z=15:

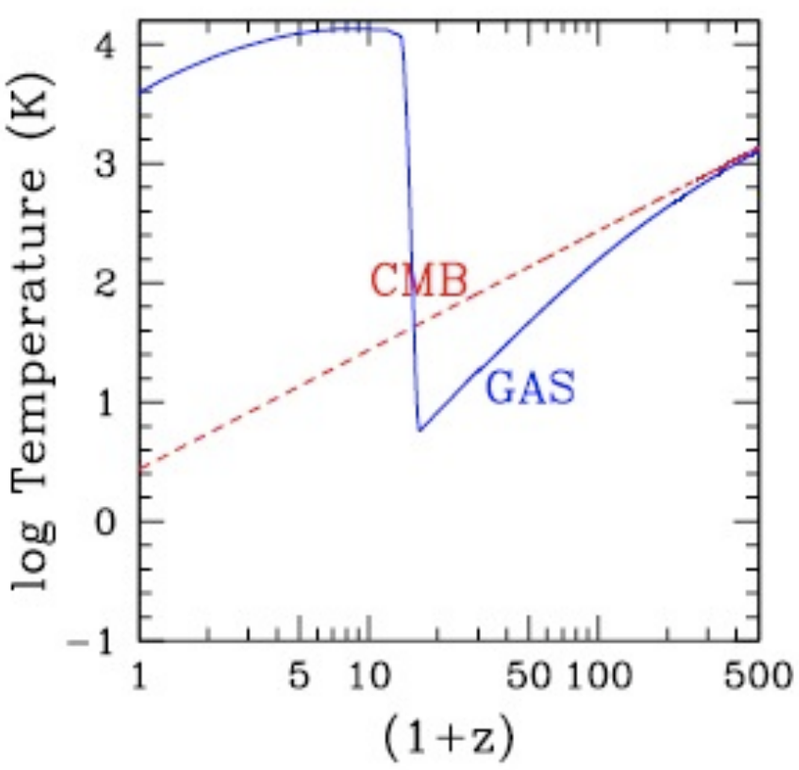

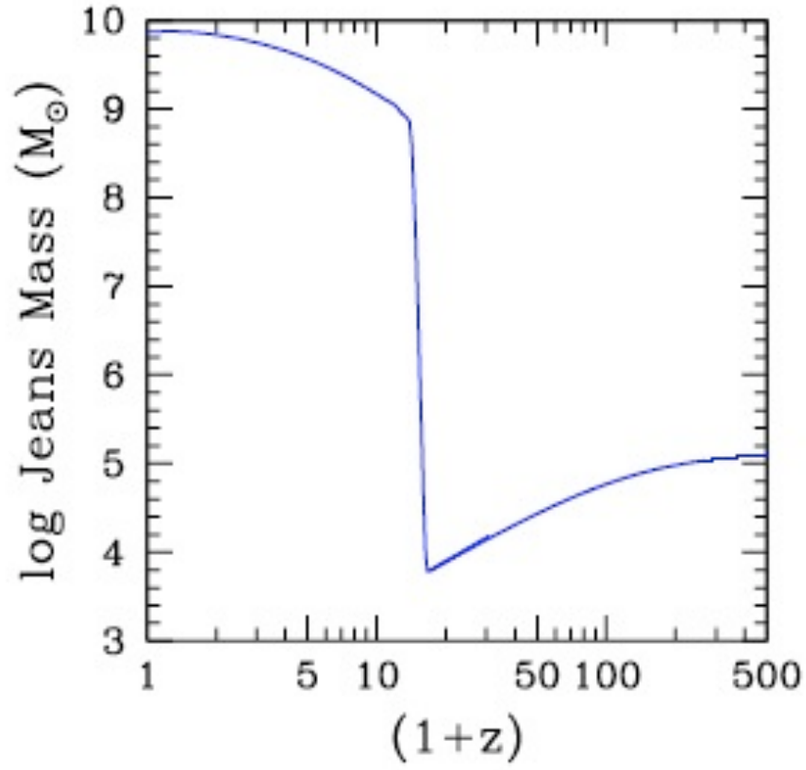

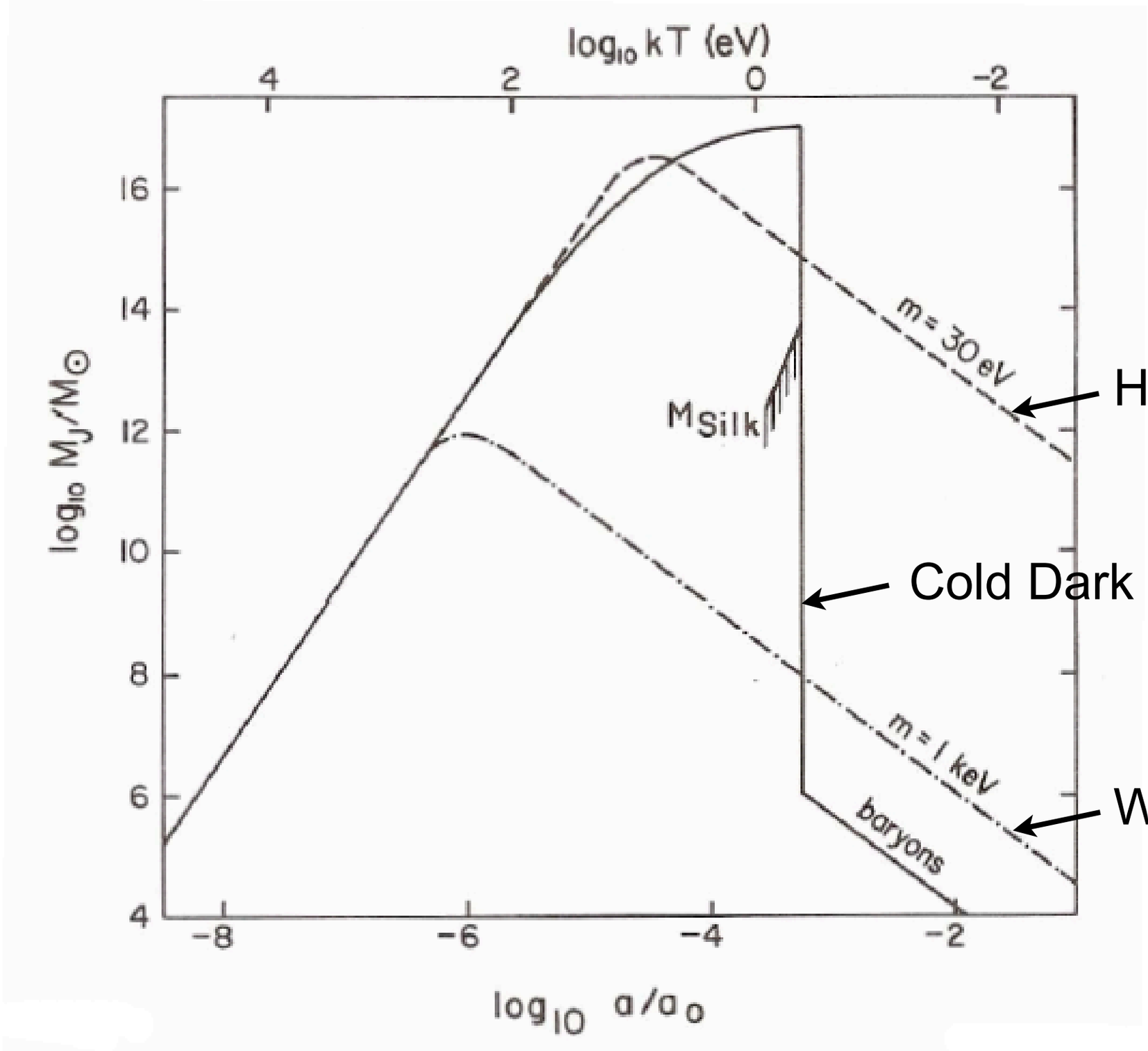

Jeans-type analysis for HDM, WDM, and CDM

GRAVITY – The Ultimate Capitalist Principle

Astronomers say that a region of the universe with more matter is "richer." Gravity magnifies differences—if one region is slightly denser than average, it will expand slightly more slowly and grow relatively denser than its surroundings, while regions with less than average density will become increasingly less dense. The rich always get richer, and the poor poorer.

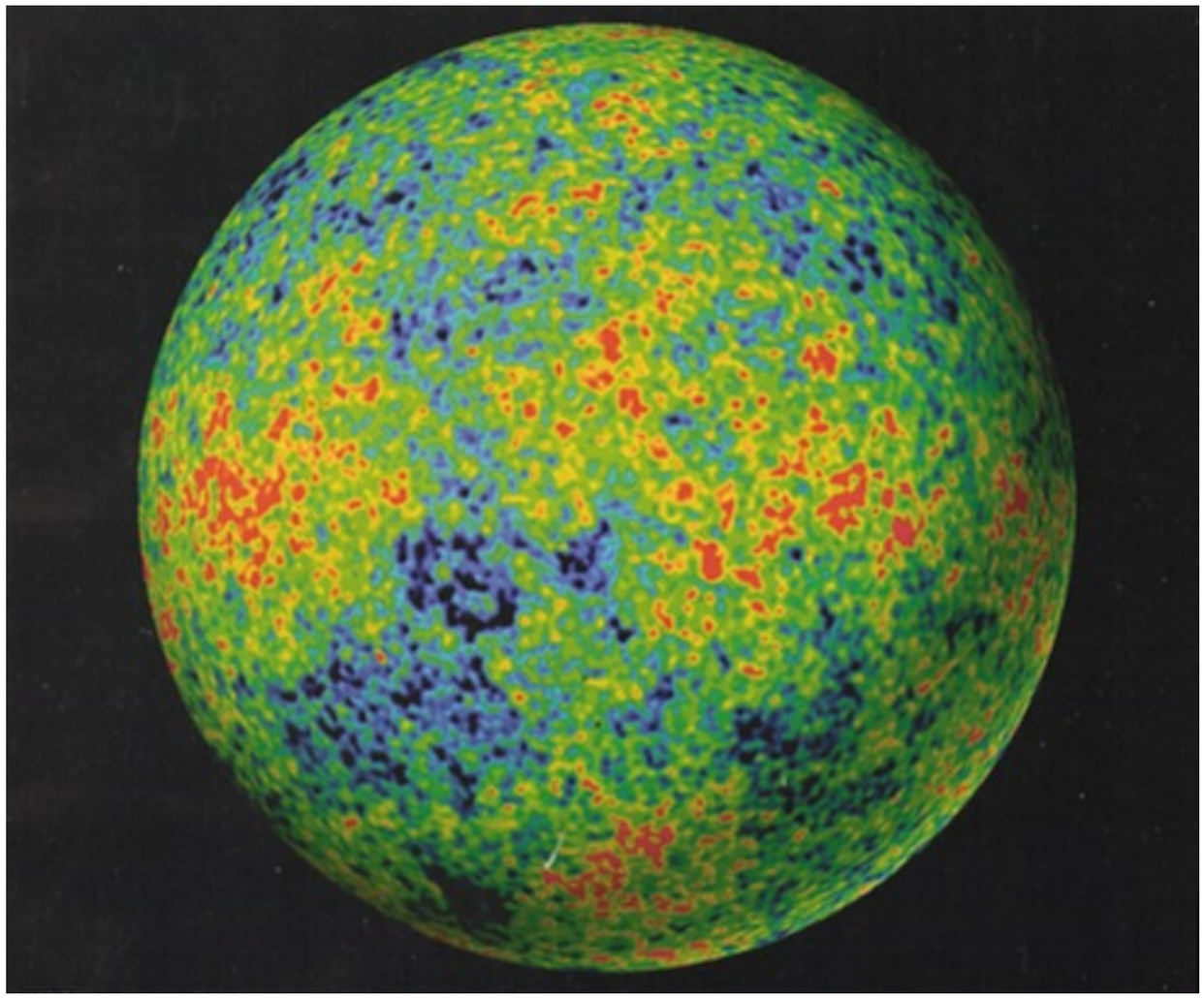

Temperature map at 380,000 years after the Big Bang. **Blue** (cooler) regions are slightly denser. From NASA's **WMAP** satellite, 2003.

The early universe expands ***almost*** perfectly uniformly. But there are small differences in density from place to place (about 30 parts per million). Because of gravity, denser regions expand more slowly, less dense regions more rapidly. Thus gravity amplifies the contrast between them, until…

Structure Formation by Gravitational Collapse

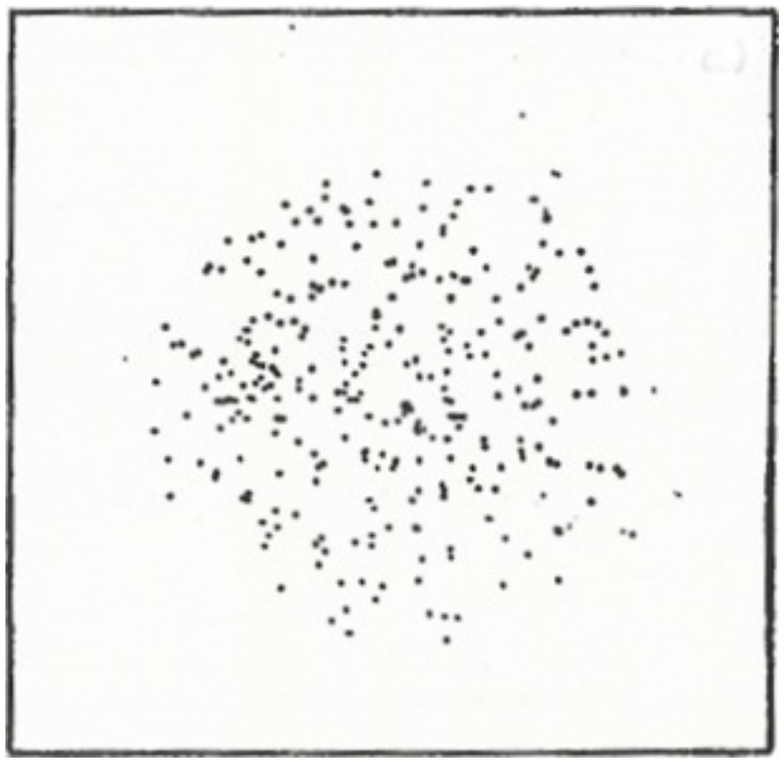

When any region becomes about twice as dense as typical regions its size, it reaches a maximum radius, ***stops expanding***,

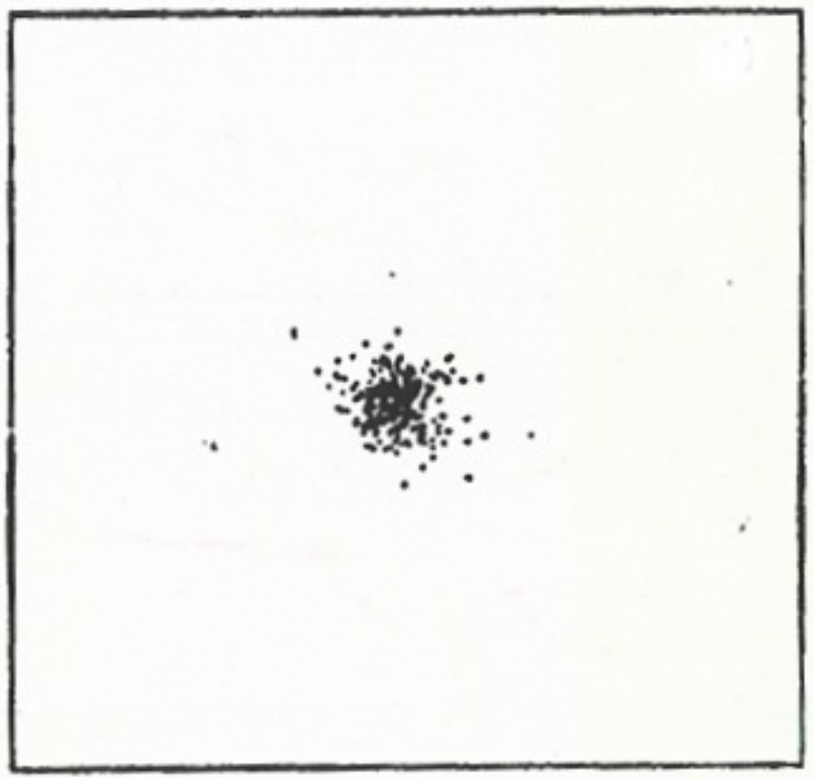

and starts falling together. The forces between the subregions generate velocities which ***prevent*** the material from ***all falling toward the center***.

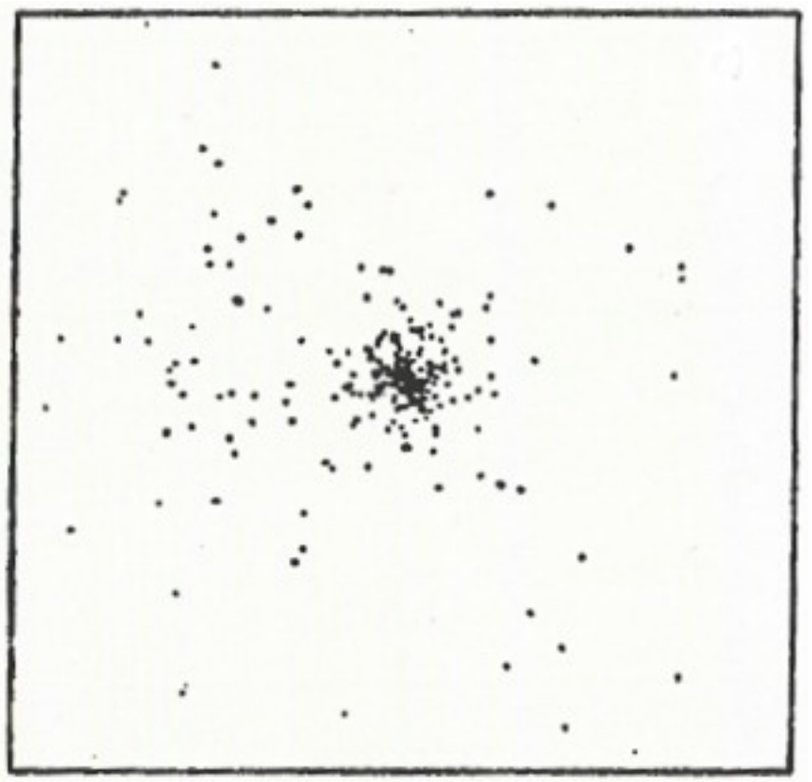

Through Violent Relaxation the dark matter quickly reaches a ***stable configuration*** that's about half the maximum radius but denser in the center.

Simulation of top-hat collapse:
P.J.E. Peebles 1970, ApJ, 75, 13.

TOP HAT
Max Expansion

VIOLENT RELAXATION

VIRIALIZED

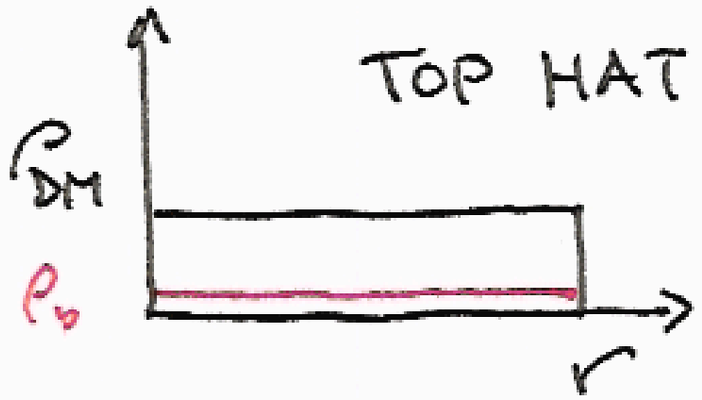

Virial Theorem: $\langle K \rangle = -\frac{1}{2}\langle W \rangle$

$W_m = \frac{G}{r_m}$, so after virialization

$$\frac{G}{r_m} = E = W + K = \frac{1}{2}\langle W \rangle = \frac{G}{2 r_v}$$

$$\Rightarrow r_v = \frac{1}{2} r_m, \quad \rho_v = 8\rho_m \approx 50\,\bar{\rho}(t_m)$$

$$\langle v^2 \rangle \approx \frac{GM}{r_v}$$

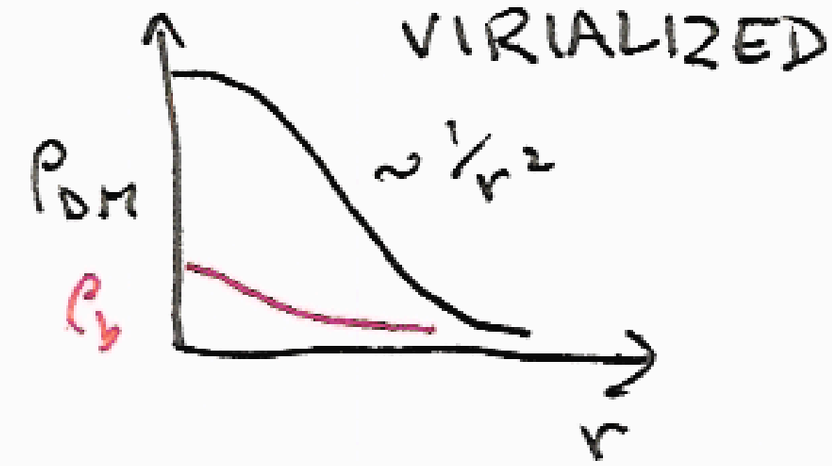

Growth and Collapse of Fluctuations

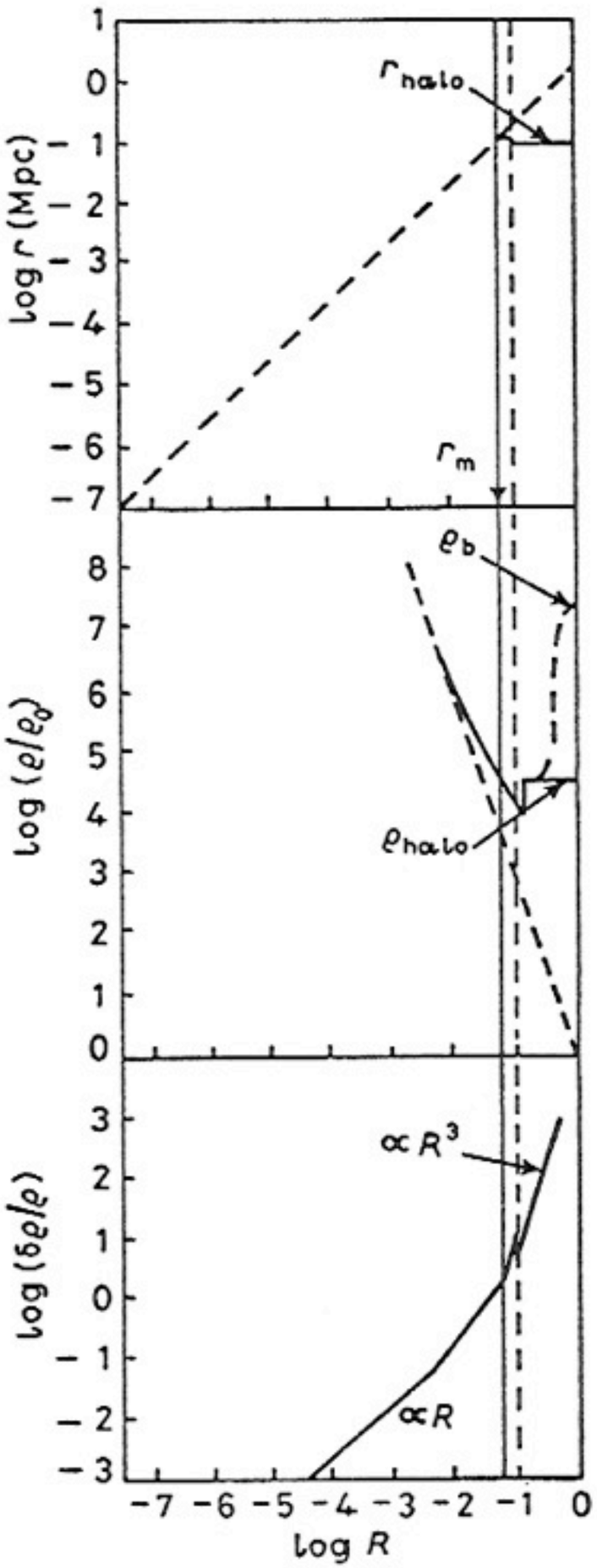

Schematic sketches of radius, density, and density contrast of an overdense fluctuation. It initially expands with the Hubble expansion, reaches a maximum radius (solid vertical line), and undergoes violent relaxation during collapse (dashed vertical line), which results in the dissipationless matter forming a stable halo. Meanwhile the ordinary matter ρb continues to dissipate kinetic energy and contract, thereby becoming more tightly bound, until dissipation is halted by star or disk formation, explaining the origin of galactic spheroids and disks.

(This was the simplified discussion of BFPR84; the figure is from my 1984 lectures at the Varenna school. Now we take into account halo growth by accretion, and the usual assumption is that spheroids form mostly as a result of galaxy mergers Toomre 1977.)

Halo and Galaxy Merging and Spheroid Formation

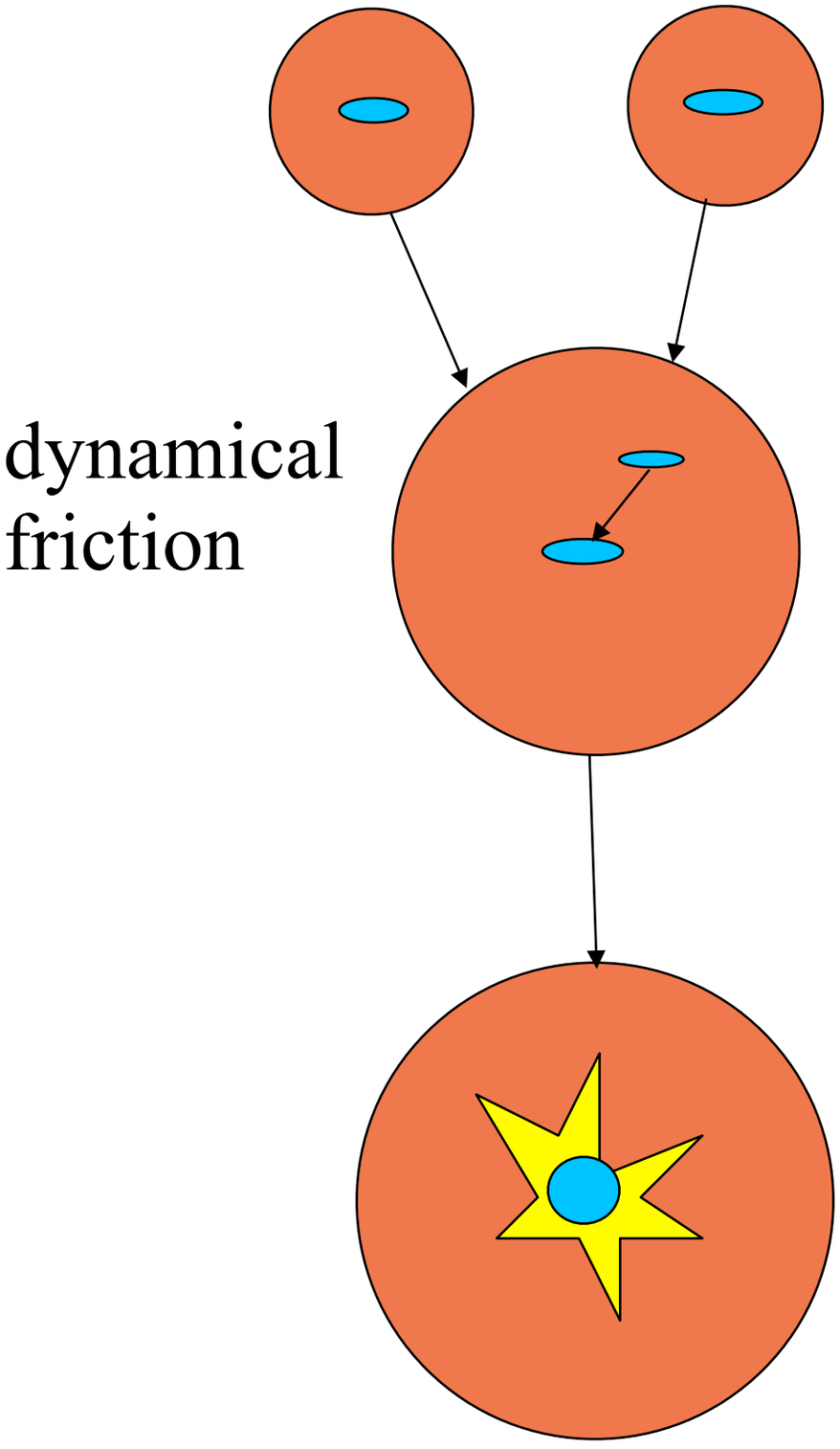

mergers can trigger starburst, forming spheroid

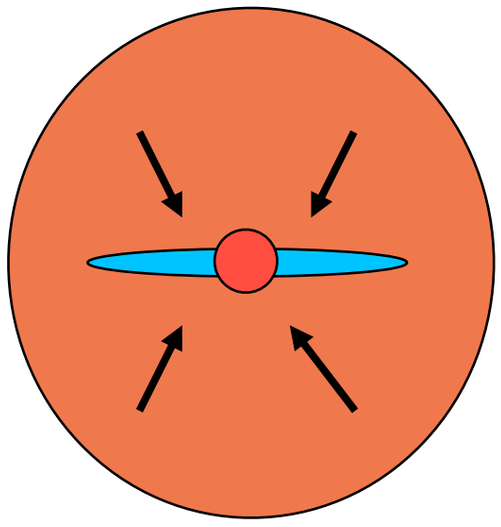

subsequent cooling forms disk

Filamentary Structure: Zel'dovich Approximation

displacement from initial position: $x(q,t) = q - D(t)\,\nabla\phi(q)$

Growth Factor

continuity: $\rho(x,t)\,d^3x = \rho_q d^3q \quad \rightarrow$

$$\rightarrow \rho(x,t) = \rho_q \,/\, \| \partial\vec{x} / \partial\vec{q} \|$$

$$= \frac{\rho_q}{(1-D(t)\lambda_1)(1-D(t)\lambda_2)(1-D(t)\lambda_3)}$$

eigenvalues of deformation tensor: $\lambda_i \equiv \frac{\partial^2\phi}{\partial^2 q_i}, \quad \lambda_1 \geq \lambda_2 \geq \lambda_3$

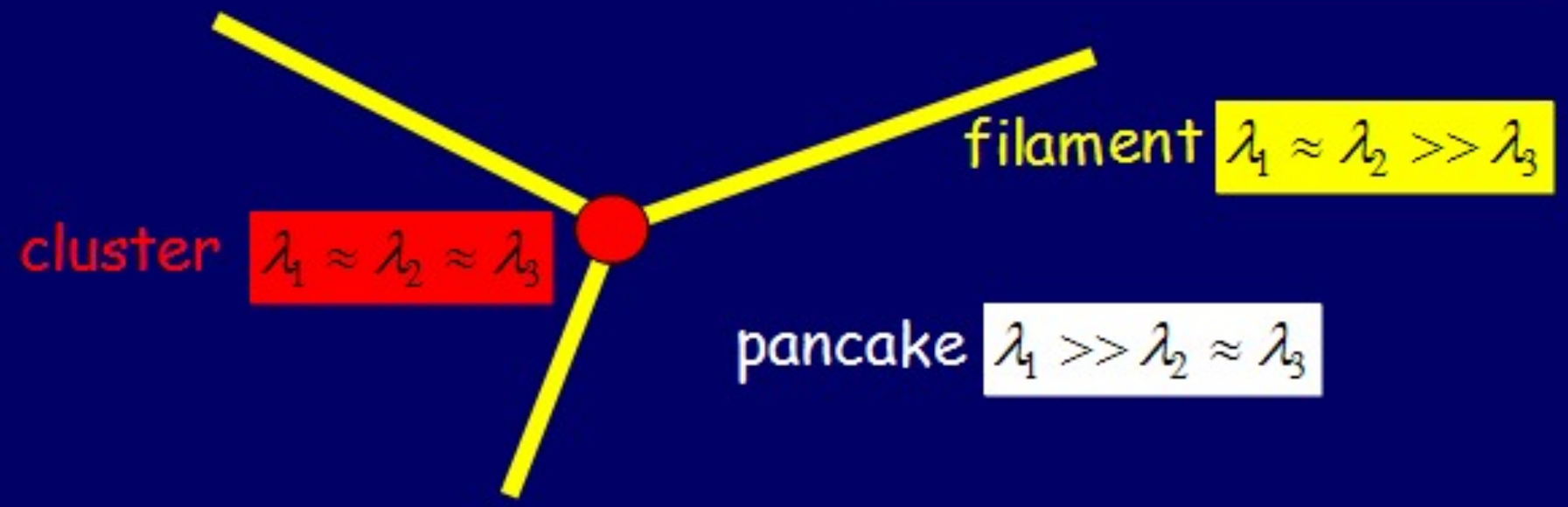

N-body simulation

ΛCDM

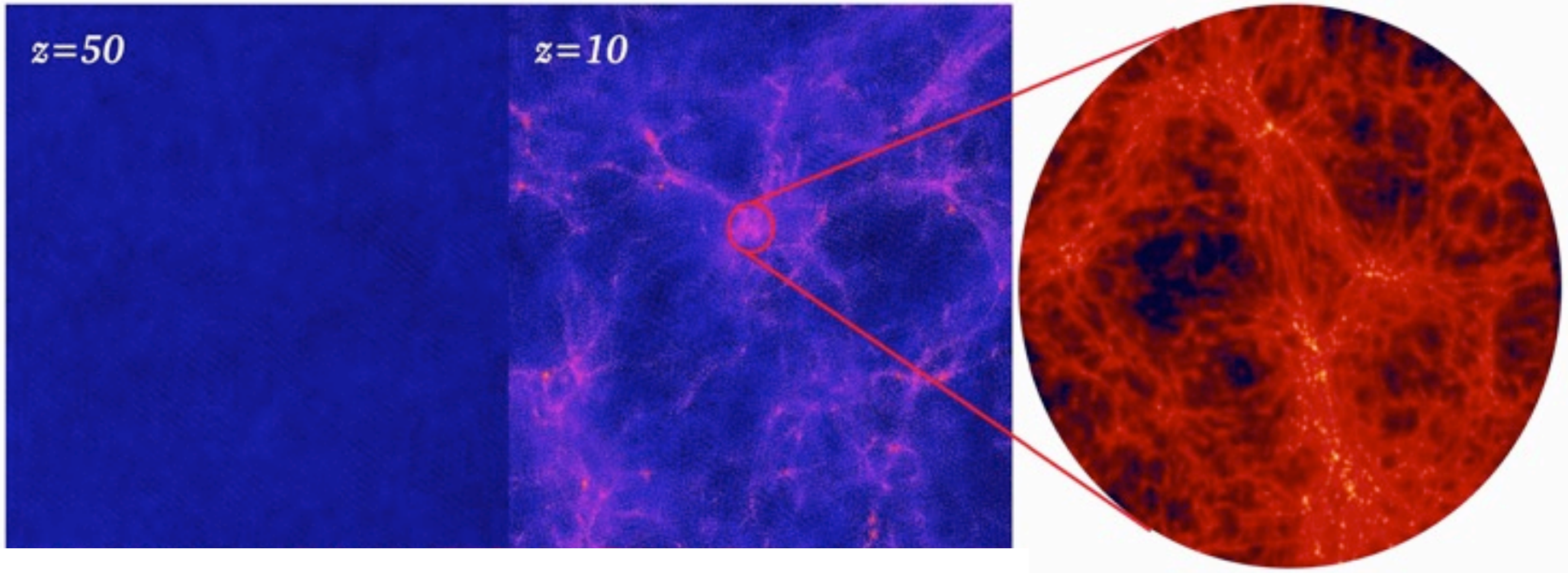
z=50
z=10

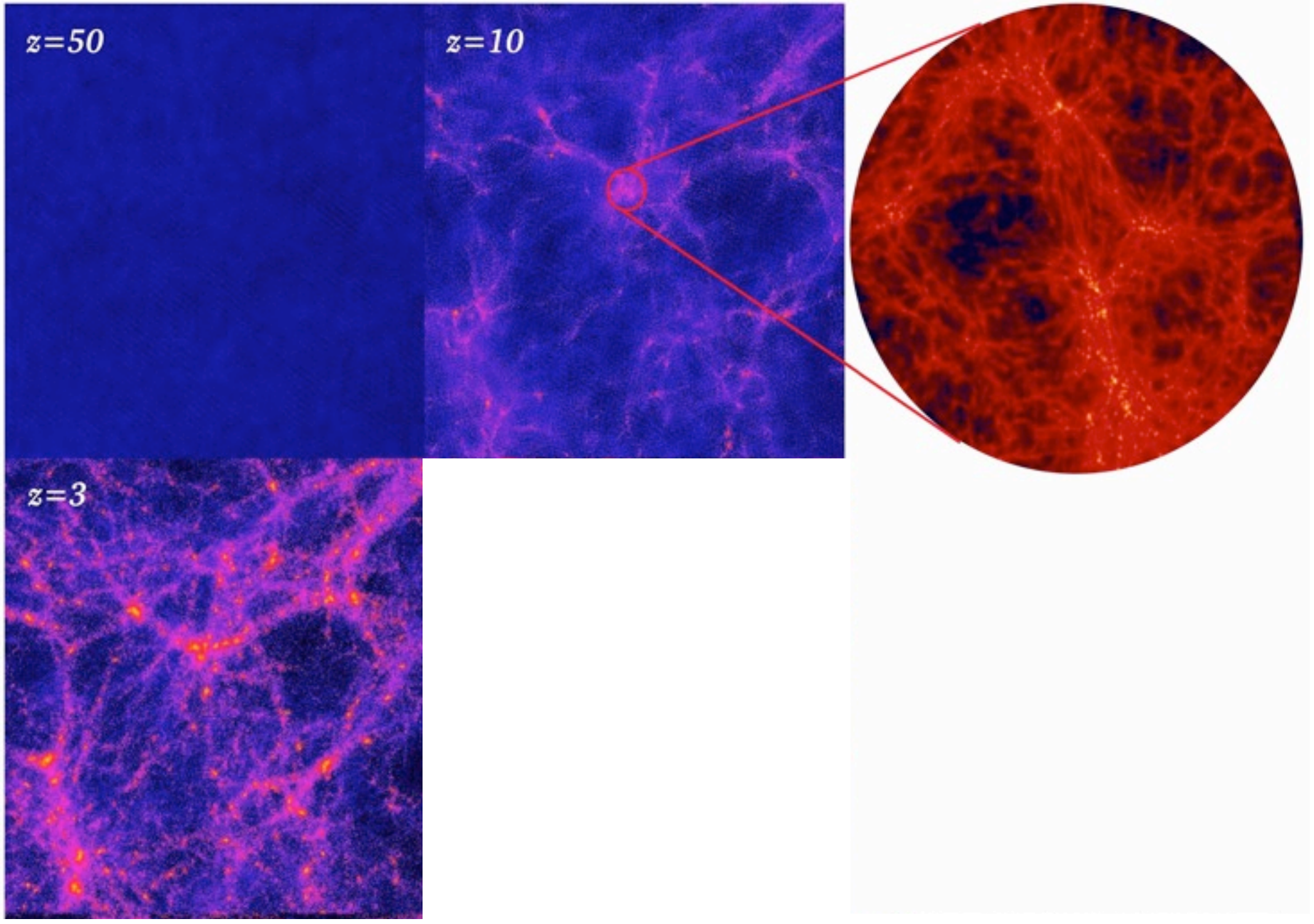
z=50
z=10
z=3

Micro-Macro Connection

Cold Dark Matter

Hot Dark Matter

ν

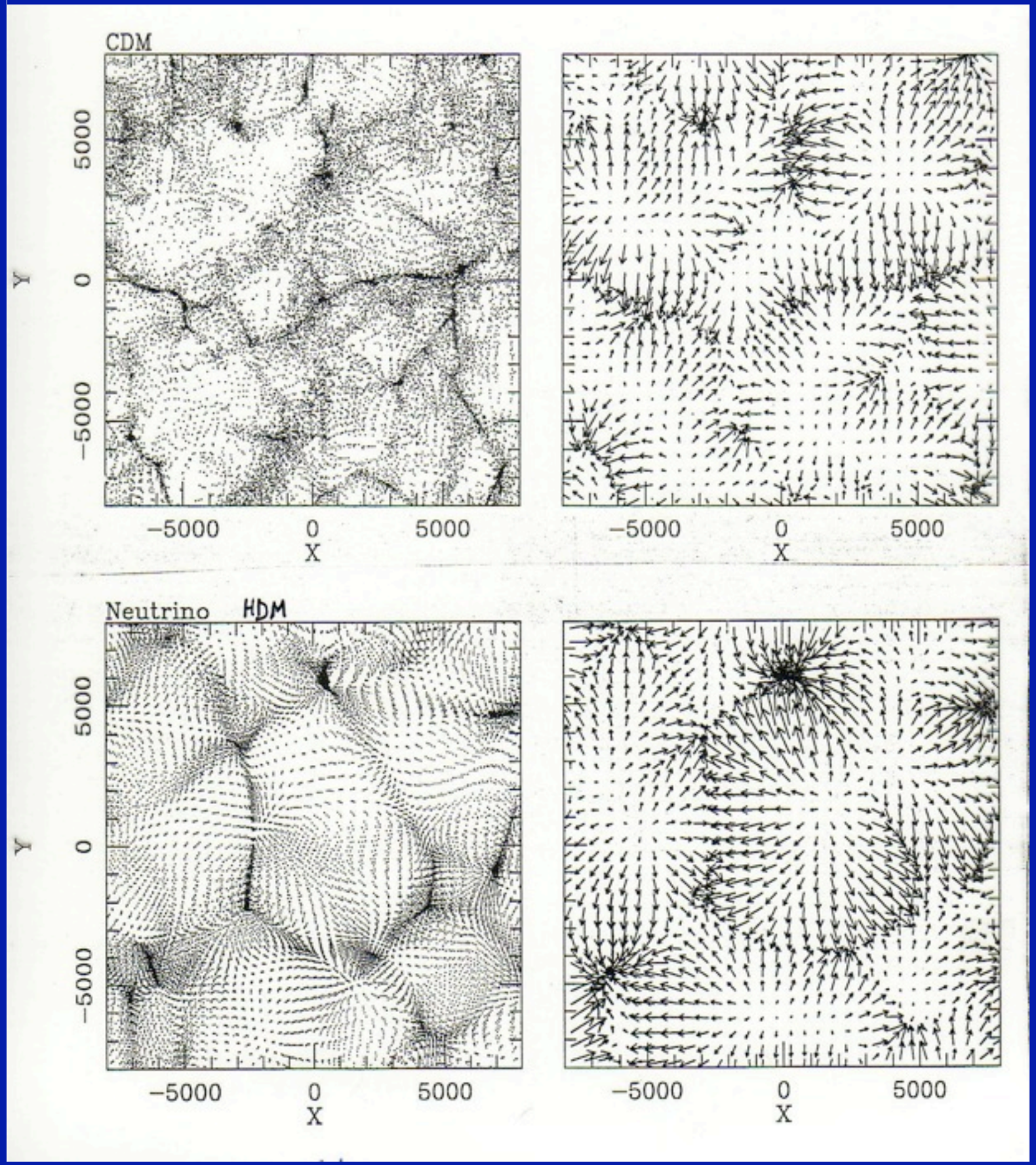

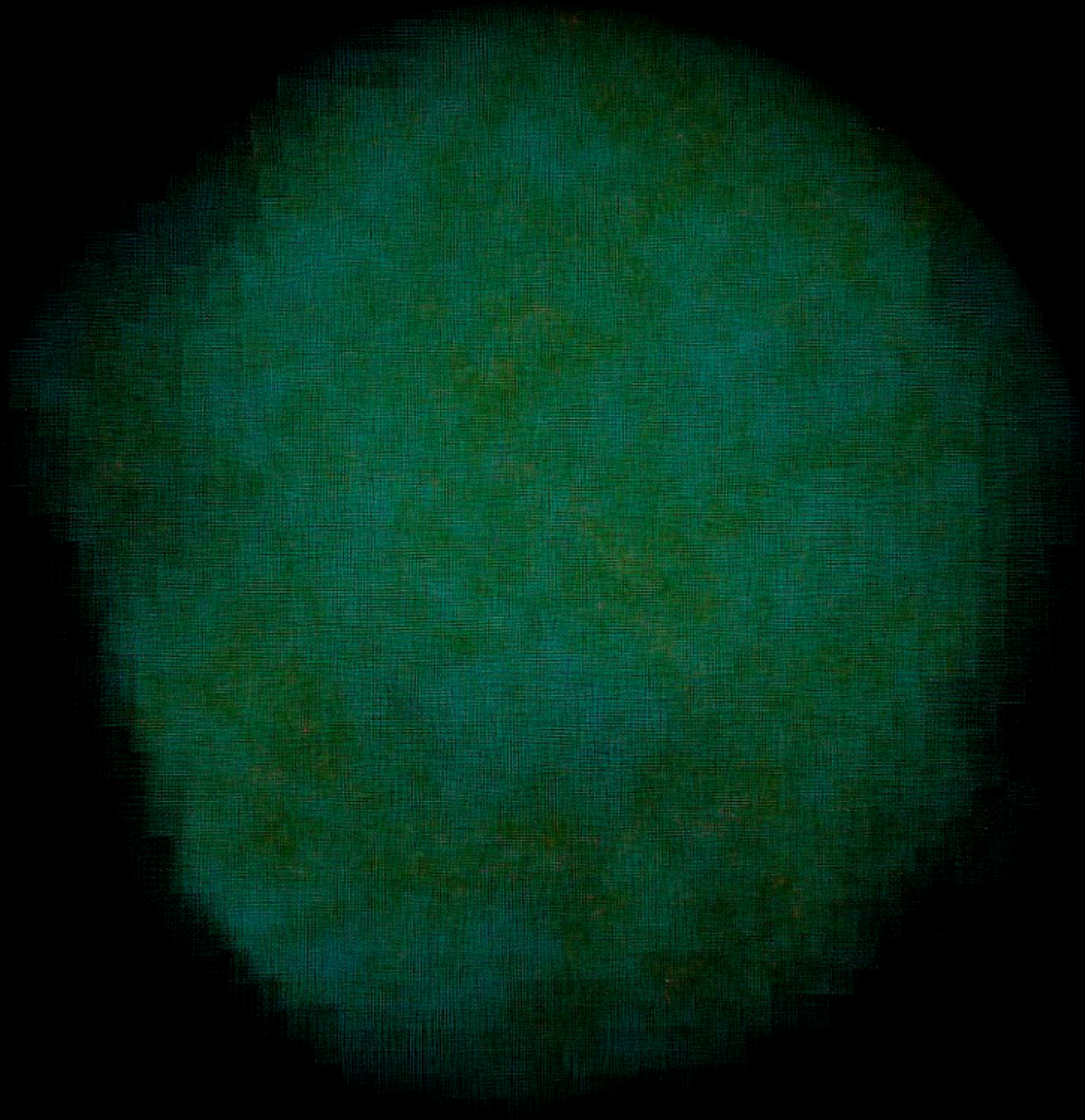

Columbia
Super
computer
NASA Ames

Simulation:
Brandon
Allgood &
Joel
Primack

Visualization:
Chris
Henze

2dF redshift survey

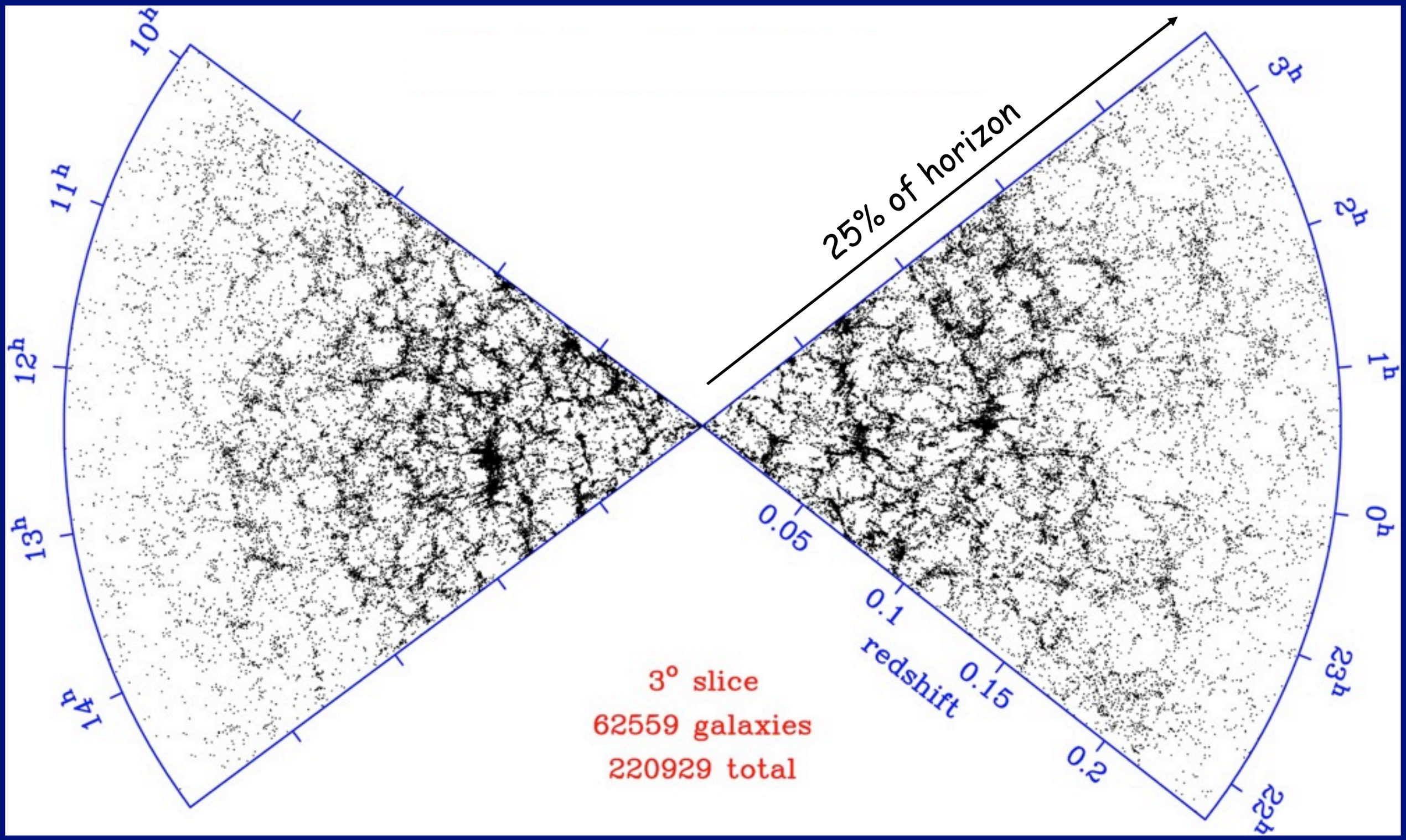

2dF and Mocks

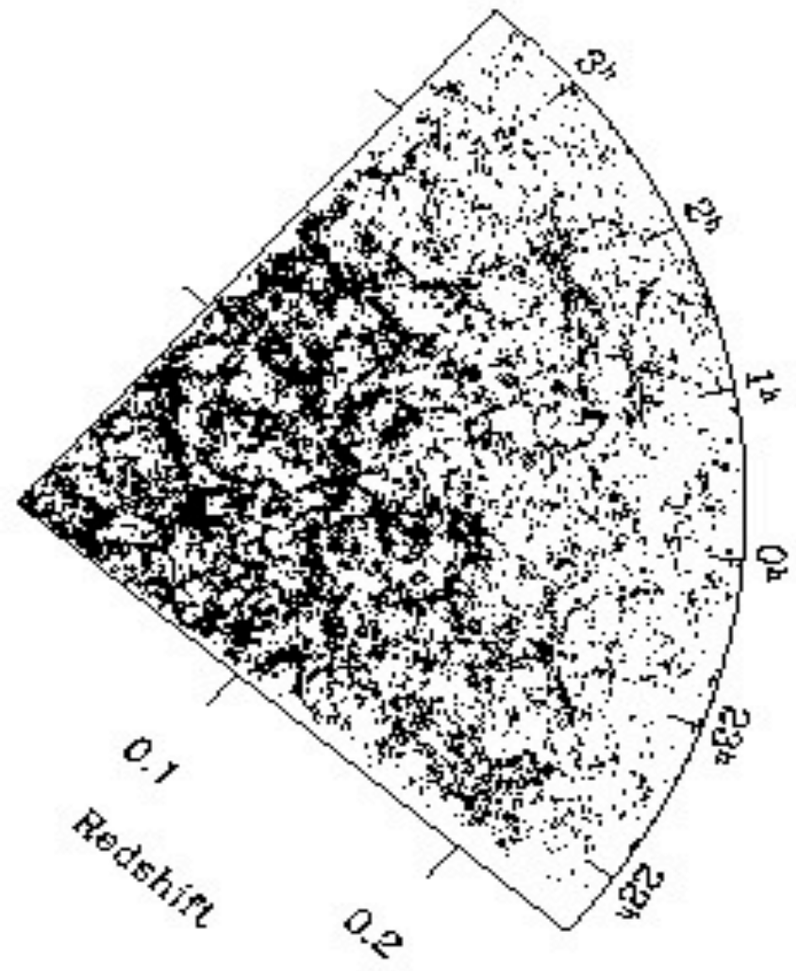

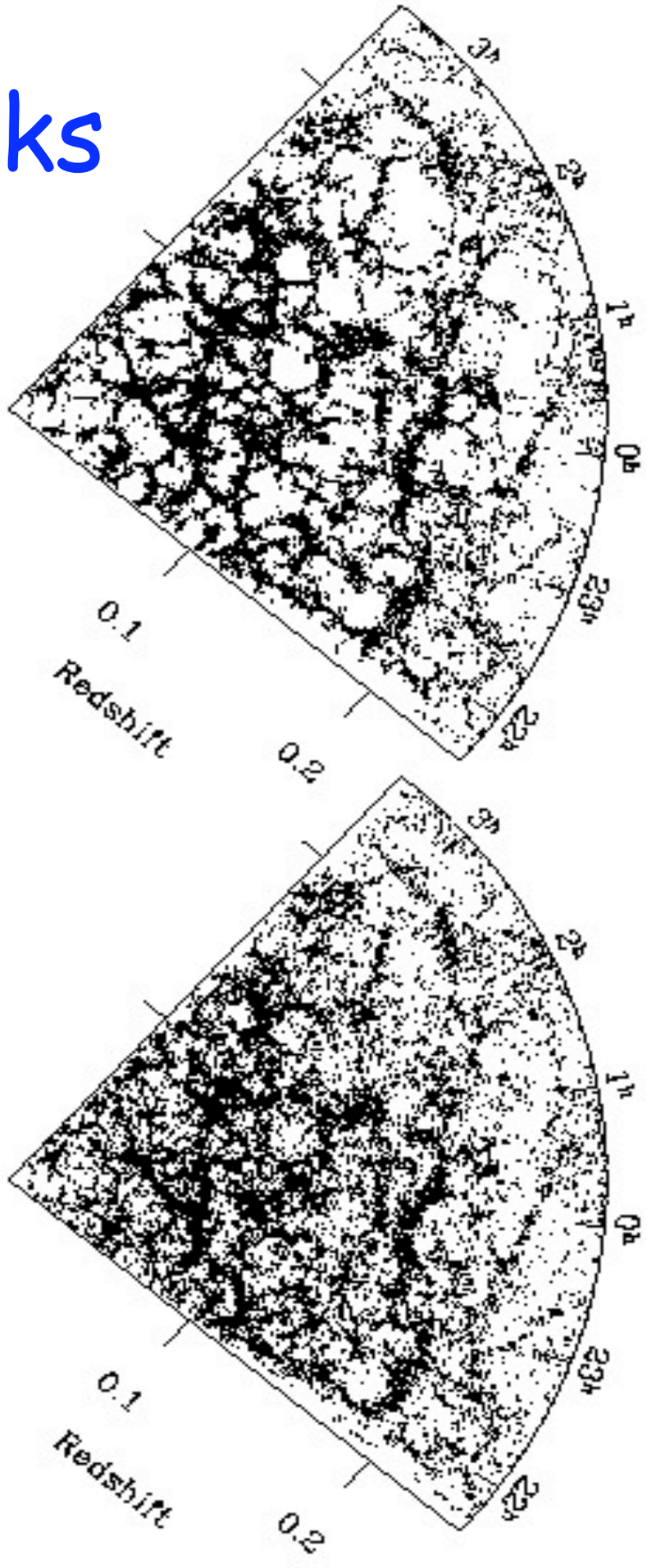

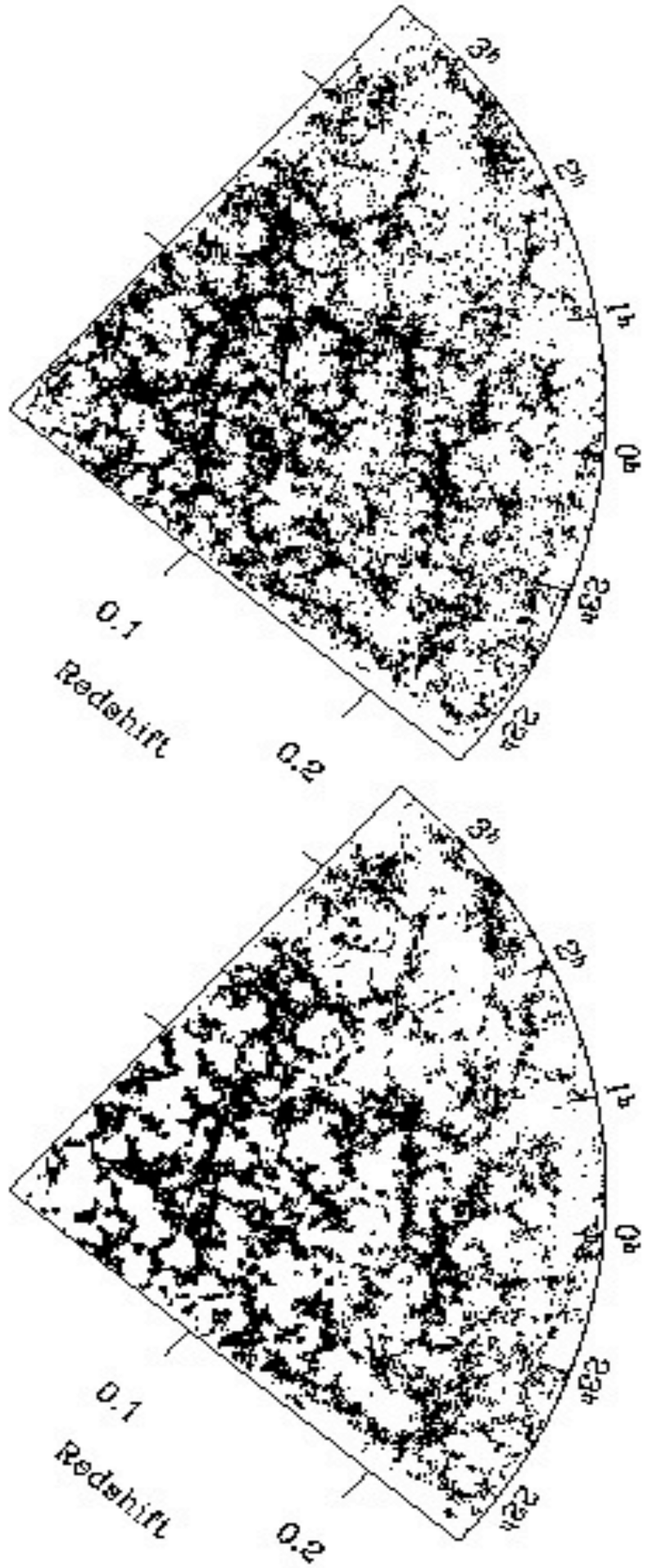

ΛCDM Fluctuation Spectrum

Agrees with Observations!

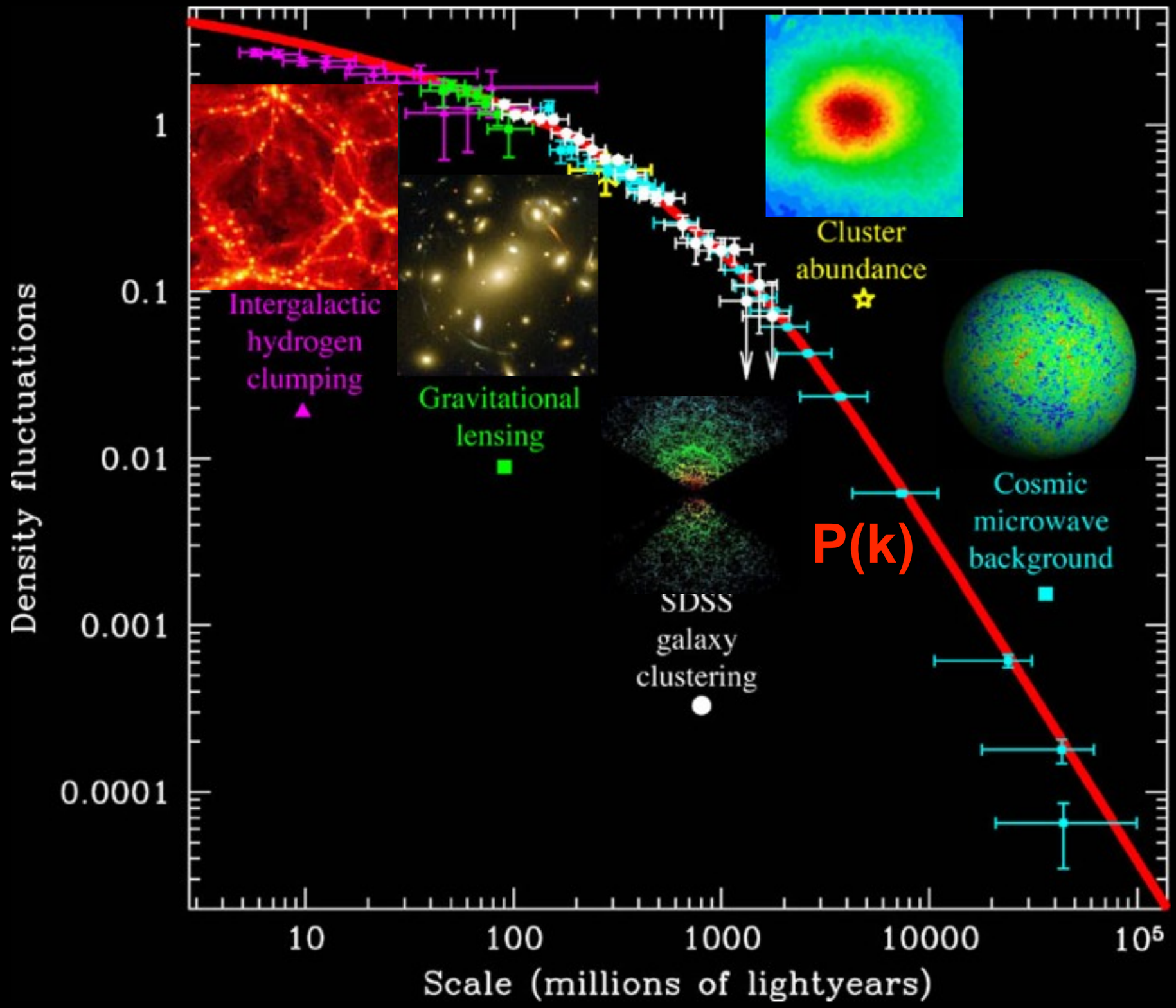

Max Tegmark

H. J. Mo, S.D.M. White
MNRAS 336 (2002) 112

The abundance and clustering of dark haloes in the standard Lambda CDM cosmogony

We define the characteristic properties of a dark halo within a sphere of radius r_{200} chosen so that the mean enclosed density is 200 times the mean cosmic value. Then

$$r_{200} = \left[\frac{GM}{100\Omega_{\rm m}(z)H^2(z)}\right]^{1/3}, \quad \text{and} \quad V_c = \left(\frac{GM}{r_{200}}\right)^{1/2}, R(M) \equiv \left(\frac{3M}{4\pi\bar{\rho}_0}\right)^{1/3}, \quad \sigma^2(R) = \frac{1}{2\pi^2}\int_0^\infty k^3 P(k)\tilde{W}^2(kR)\frac{{\rm d}k}{k},$$

According to the argument first given by Press & Schechter (1974, hereafter PS), the abundance of haloes as a function of mass and redshift, expressed as the number of haloes per unit comoving volume at redshift z with mass in the interval $(M, M + dM)$, may be written as

$$n(M,z){\rm d}M = \sqrt{\frac{2}{\pi}}\frac{\bar{\rho}_0}{M}\frac{{\rm d}\nu}{{\rm d}M}\exp\left(-\frac{\nu^2}{2}\right){\rm d}M\,. \tag{9}$$

Here $\nu \equiv \delta_c/[D(z)\sigma(M)]$, where $\delta_c \approx 1.69$ and the growth factor is $D(z) = g(z)/[g(0)(1+z)]$ with

$$g(z) \approx \frac{5}{2}\Omega_{\rm m}\left[\Omega_{\rm m}^{4/7} - \Omega_\Lambda + (1+\Omega_{\rm m}/2)(1+\Omega_\Lambda/70)\right]^{-1}, \ \Omega_{\rm m} \equiv \Omega_{\rm m}(z), \quad \Omega_\Lambda \equiv \Omega_\Lambda(z) = \frac{\Omega_{\Lambda,0}}{E^2(z)}.$$

$$E(z) = \left[\Omega_{\Lambda,0} + (1-\Omega_0)(1+z)^2 + \Omega_{{\rm m},0}(1+z)^3\right]^{\frac{1}{2}}.$$

Lahav, Lilje, Primack, & Rees 1991

Press & Schechter derived the above mass function from the *Ansatz* that the fraction F of all cosmic mass which at redshift z is in haloes with masses exceeding M is *twice* the fraction of randomly placed spheres of radius $R(M)$ which have linear overdensity at that time exceeding δ_c, the value at which a spherical perturbation collapses. Since the linear fluctuation distribution is gaussian this hypothesis implies

$$F(>M,z) = {\rm erfc}\left(\frac{\nu}{\sqrt{2}}\right), \tag{12}$$

and equation (9) then follows by differentiation.

The PS formula is $$n(M,z)\mathrm{d}M = \sqrt{\frac{2}{\pi}}\frac{\bar{\rho}_0}{M}\frac{\mathrm{d}\nu}{\mathrm{d}M}\exp\left(-\frac{\nu^2}{2}\right)\mathrm{d}M \quad (9)$$

Numerical simulations show that although the scaling properties implied by the PS argument hold remarkably well for a wide variety of hierarchical cosmogonies, substantially better fits to simulated mass functions are obtained if the error function in equation (12) is replaced by a function of slightly different shape. Sheth & Tormen (1999) suggested the following modification of equation (9)

$$n(M,z)\mathrm{d}M = A\left(1+\frac{1}{\nu'^{2q}}\right)\sqrt{\frac{2}{\pi}}\frac{\bar{\rho}}{M}\frac{\mathrm{d}\nu'}{\mathrm{d}M}\exp\left(-\frac{\nu'^2}{2}\right)\mathrm{d}M, \quad (14)$$

where $\nu' = \sqrt{a}\nu$, $a = 0.707$, $A \approx 0.322$ and $q = 0.3$.

[See Sheth, Mo & Tormen (2001) and Sheth & Tormen (2002) for a justification of this formula in terms of an ellipsoidal model for perturbation collapse.] The fraction of all matter in haloes with mass exceeding M can be obtained by integrating equation (14). To good approximation,

$$F(>M,z) \approx 0.4\left(1+\frac{0.4}{\nu^{0.4}}\right)\mathrm{erfc}\left(\frac{0.85\nu}{\sqrt{2}}\right)$$

In a detailed comparison with a wide range of simulations, Jenkins et al. (2001) confirmed that this model is indeed a good fit provided haloes are defined at the same density contrast relative to the mean in all cosmologies. This is for FOF halo finding -- but Klypin, Trujillo, Primack 2010 find that the more physical Bound Density Maximum (BDM) halo finder results in 10x lower halo number density at z=10.

Sheth-Tormen Fails at High Redshifts

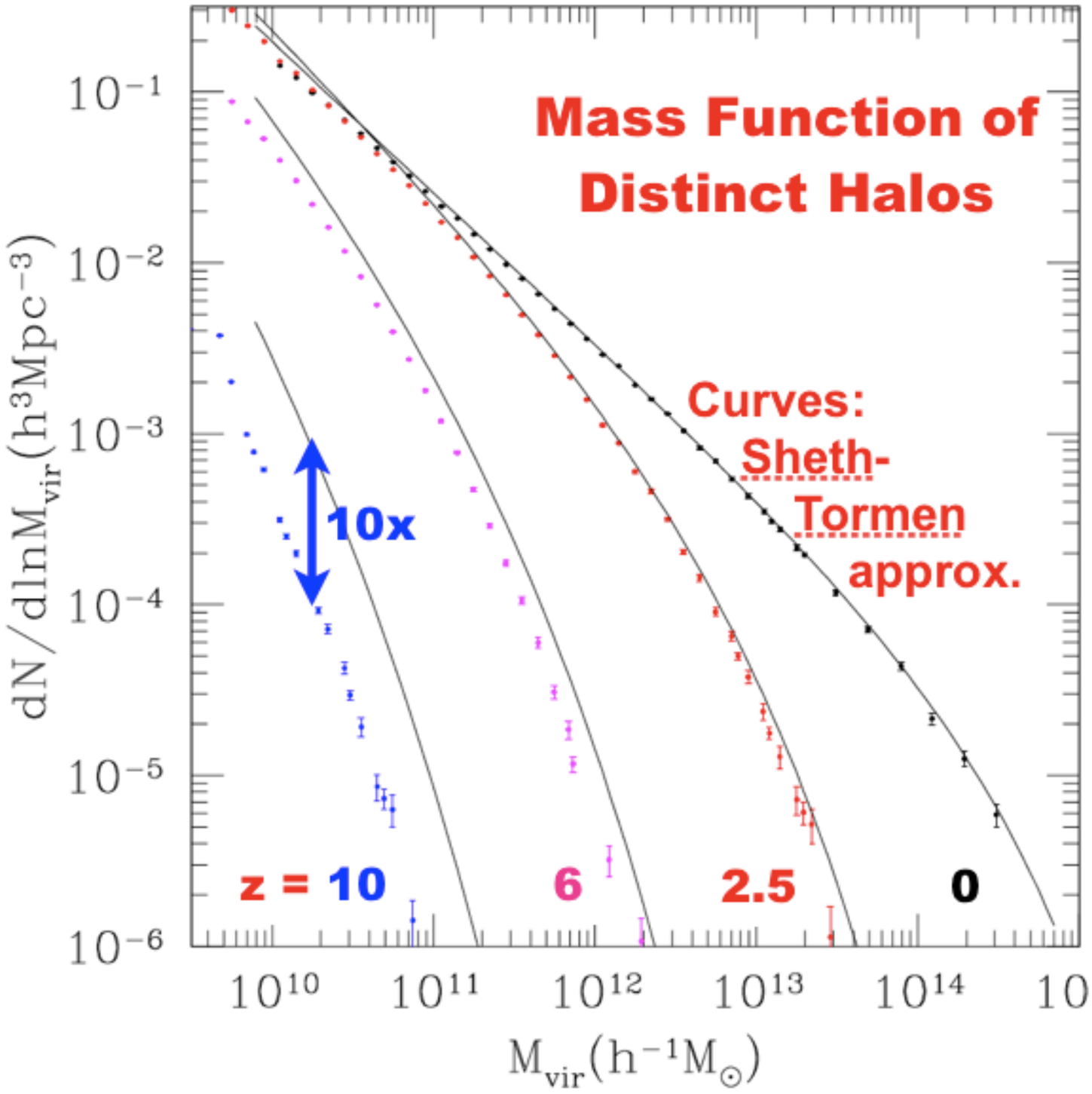

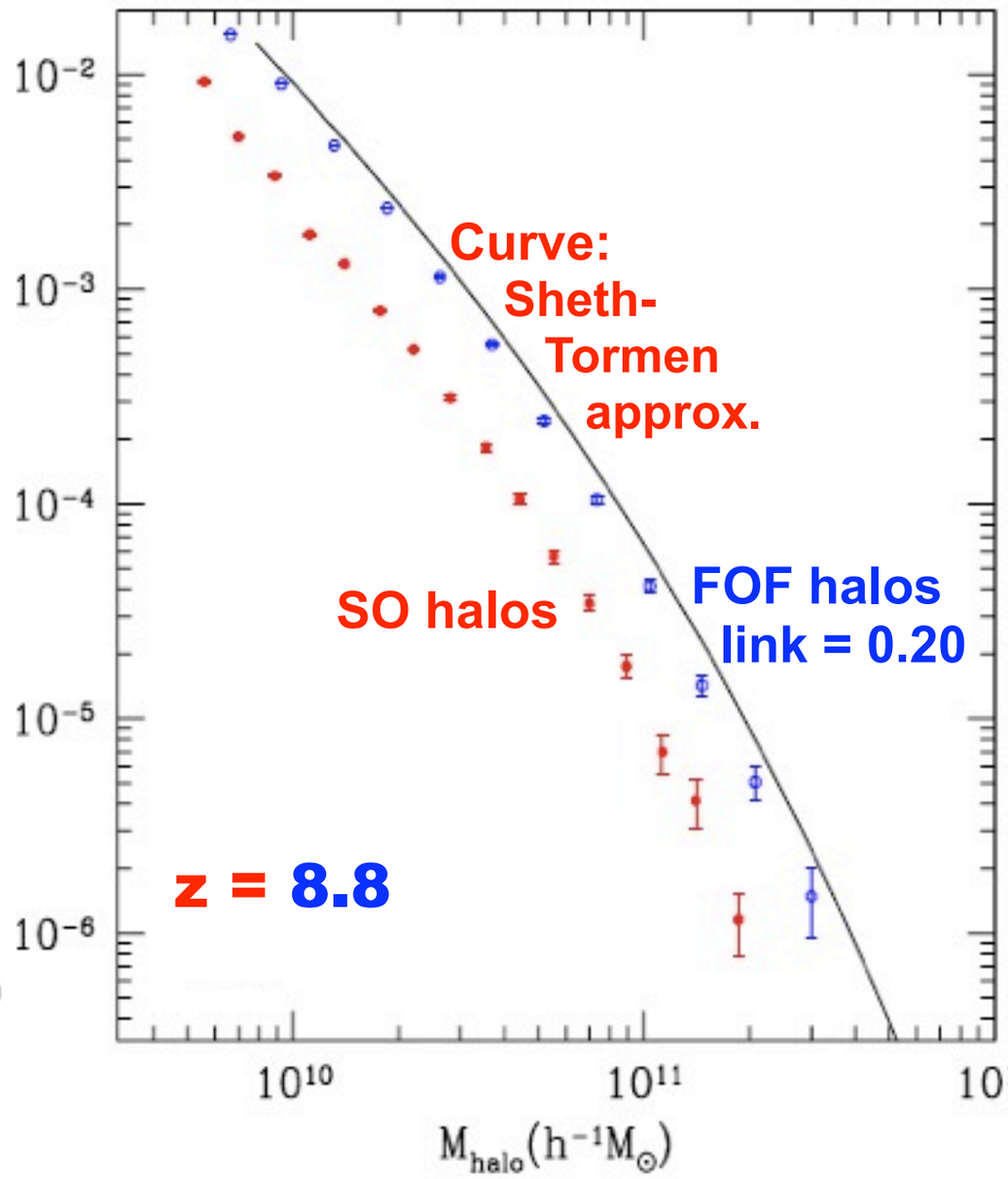

Sheth-Tormen approximation with the same WMAP5 parameters used for Bolshoi simulation very accurately agrees with abundance of halos at low redshifts, but increasingly overpredicts bound spherical overdensity halo abundance at higher redshifts.

Klypin, Trujillo, & Primack, arXiv: 1002.3660v3

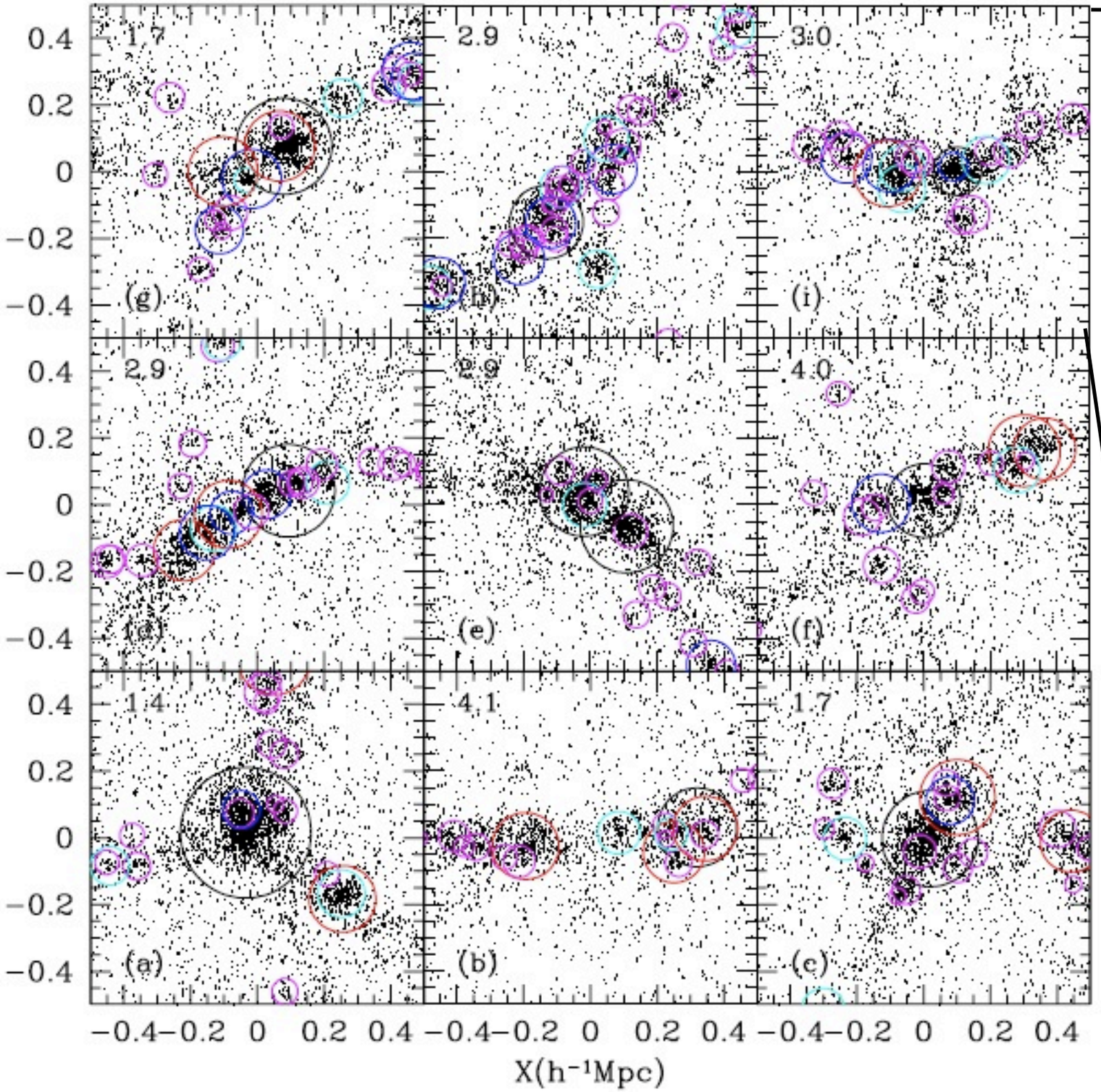

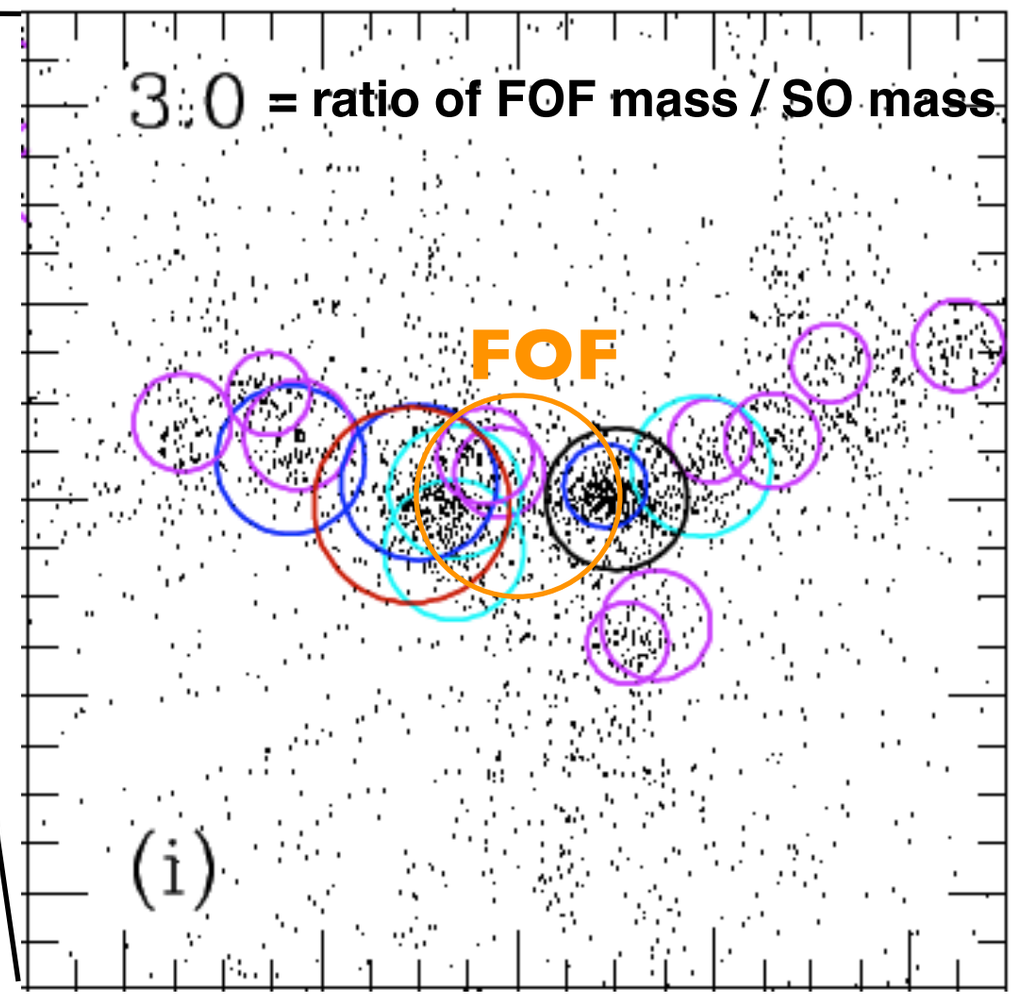

FOF linked together a chain of halos that formed in long and dense filaments (also in panels b, d, f, h; e = major merger)

Each panel shows 1/2 of the dark matter particles in cubes of $1h^{-1}$ Mpc size. The center of each cube is the exact position of the center of mass of the corresponding FOF halo. The effective radius of each FOF halo in the plots is 150 – 200 h^{-1} kpc. Circles indicate virial radii of distinct halos and subhalos identified by the spherical overdensity algorithm BDM.

Klypin, Trujillo, & Primack, arXiv: 1002.3660v3

Comoving Halo Number Density $n(M_{halo})$

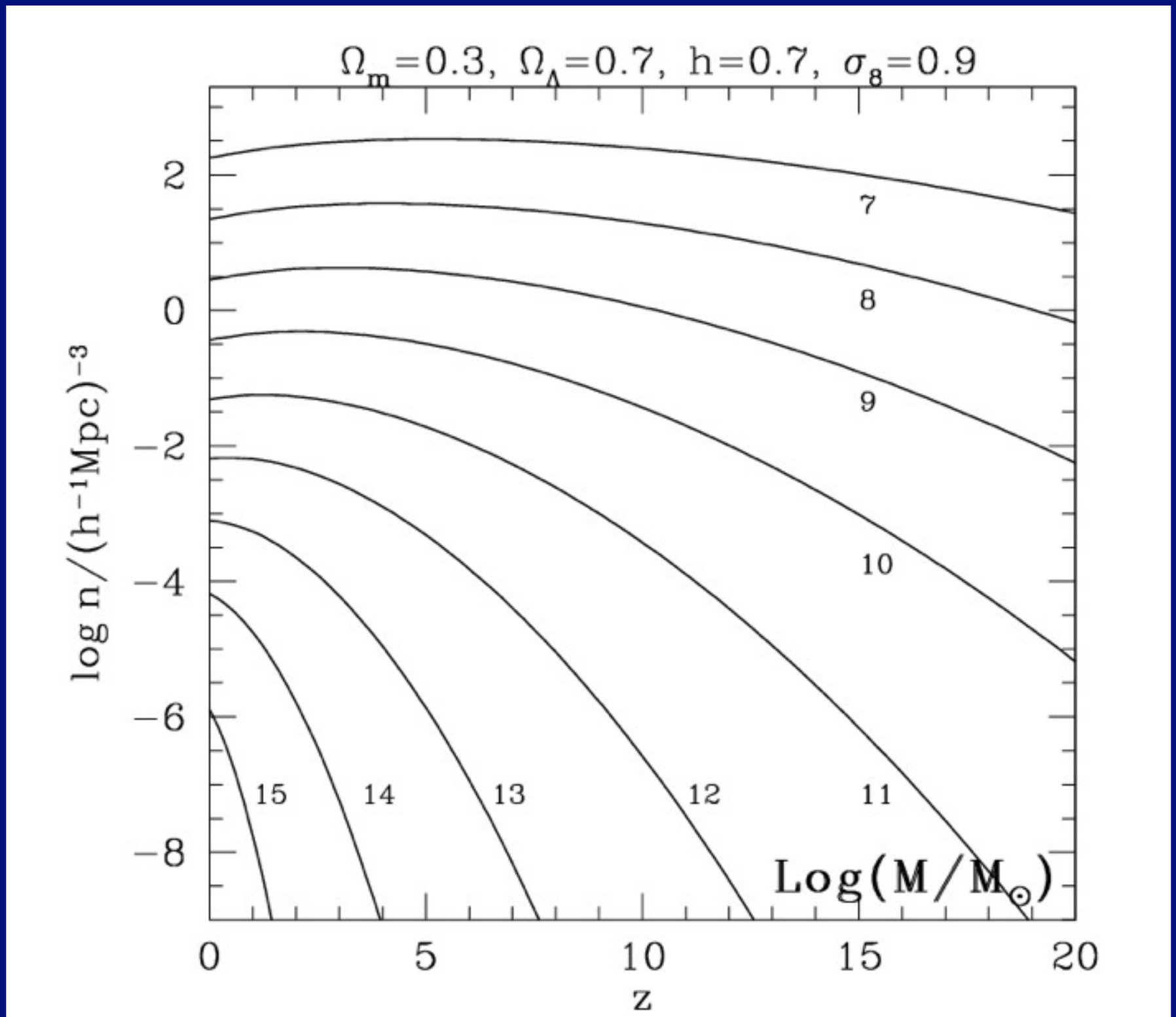

Mo & White 2002

Comoving Halo Number Density n(M_{halo})

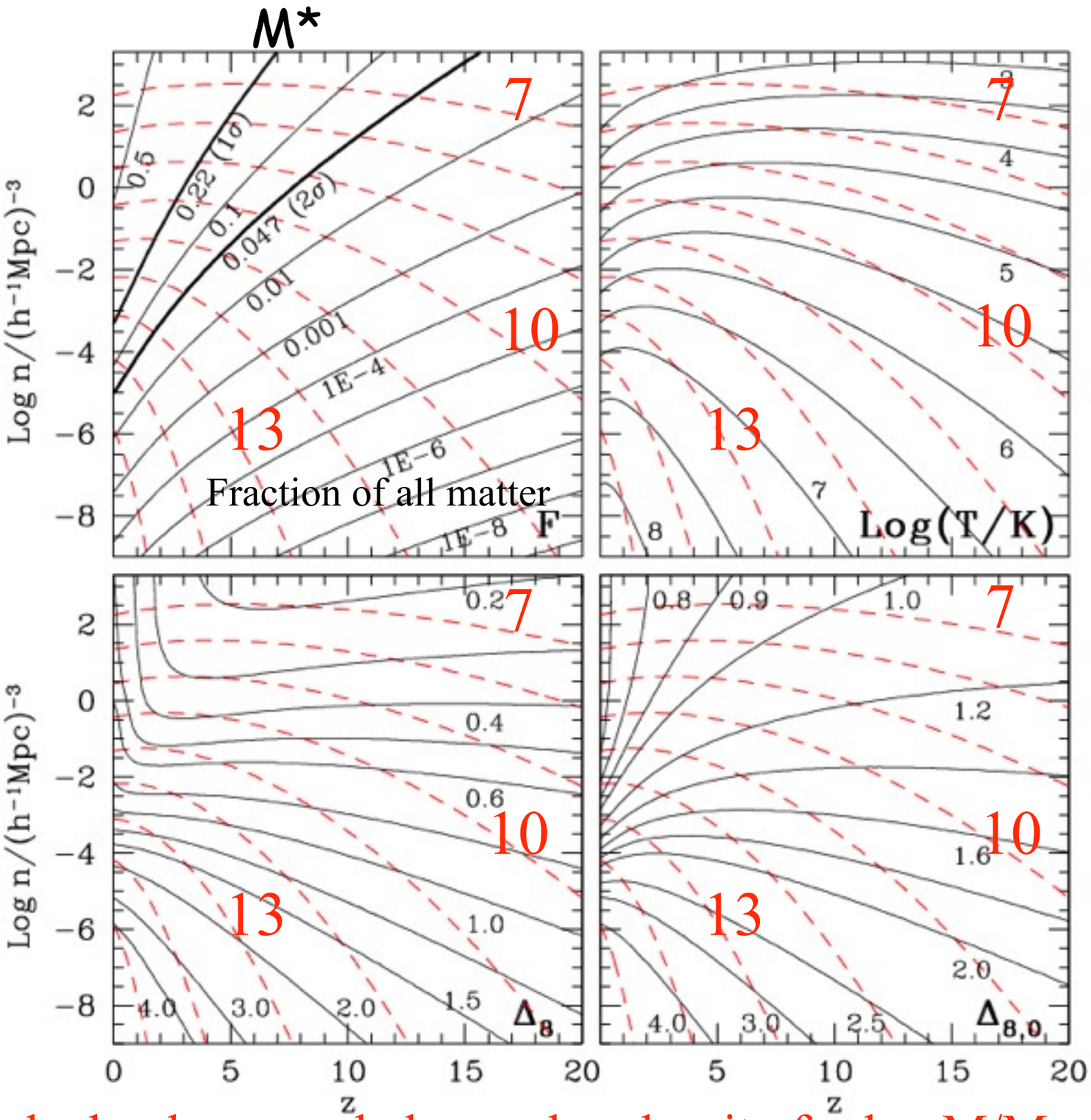

Dashed red curves: halo number density for log M/M_{sun}

Standard LCDM

Mo & White 2002

Cosmological Simulation Methods

Dissipationless Simulations

Particle-Particle (PP) - Aarseth NbodyN, N=1,...,6
Particle Mesh (PM) - see Klypin & Holtzman 1997
Adaptive PM (P3M) - Efstathiou et al.
Tree - Barnes & Hut 1986, PKDGRAV Stadel
TreePM - GADGET2, Springel 2005
Adaptive Mesh Refinement (AMR) - Klypin (ART)

Hydrodynamical Simulations

Fixed grid - Cen & Ostriker
Smooth Particle Hydrodynamics (SPH) - GADGET2, Springel 2005
- Gasoline, Wadsley, Stadel, & Quinn
Adaptive grid - ART+hydro - Klypin & Kravtsov

Initial Conditions

Standard: Gaussian P(k) realized uniformly, Zel'dovich displacement
Multimass - put lower mass particles in a small part of sim volume
Constrained realization - small scale: simulate individual halos (NFW)
large scale: simulate particular region

Reviews

Bertschinger ARAA 1998, Klypin lectures 2002, U Washington website

Structure of Dark Matter Halos

Navarro, Frenk, White

1996 1997 ⟶

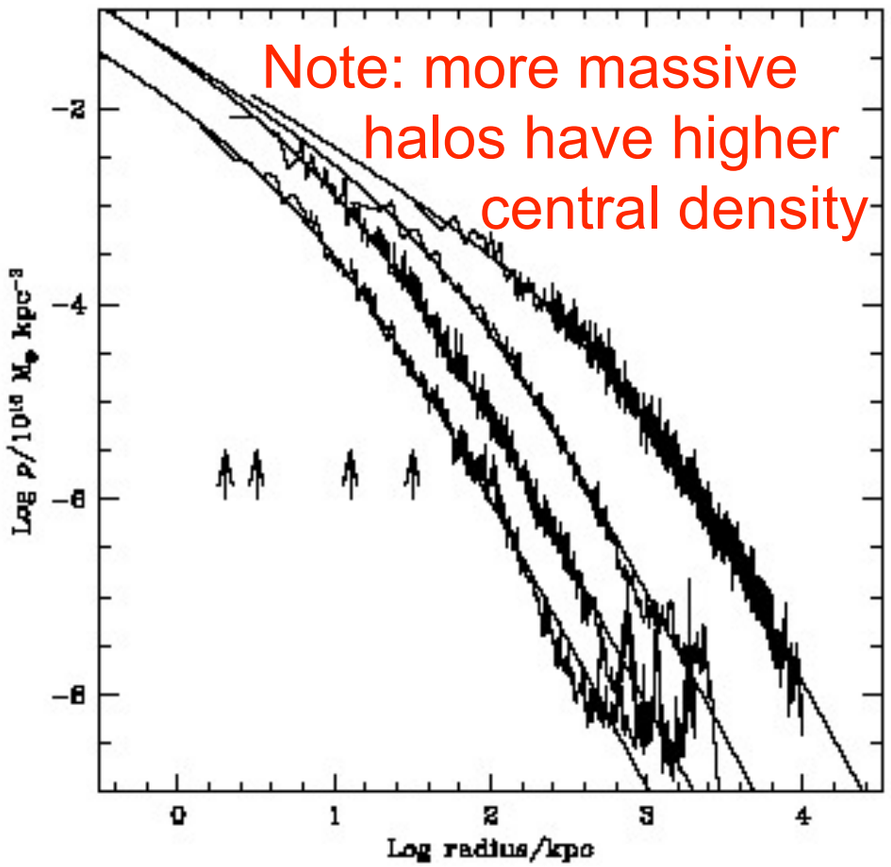

Fig. 3.— Density profiles of four halos spanning four orders of magnitude in mass. The arrows indicate the gravitational softening, h_g, of each simulation. Also shown are fits from eq.3. The fits are good over two decades in radius, approximately from h_g out to the virial radius of each system.

$$\frac{\rho(r)}{\rho_{crit}} = \frac{\delta_c}{(r/r_s)(1+r/r_s)^2}, \qquad (3)$$

NFW formula works for <u>all</u> models

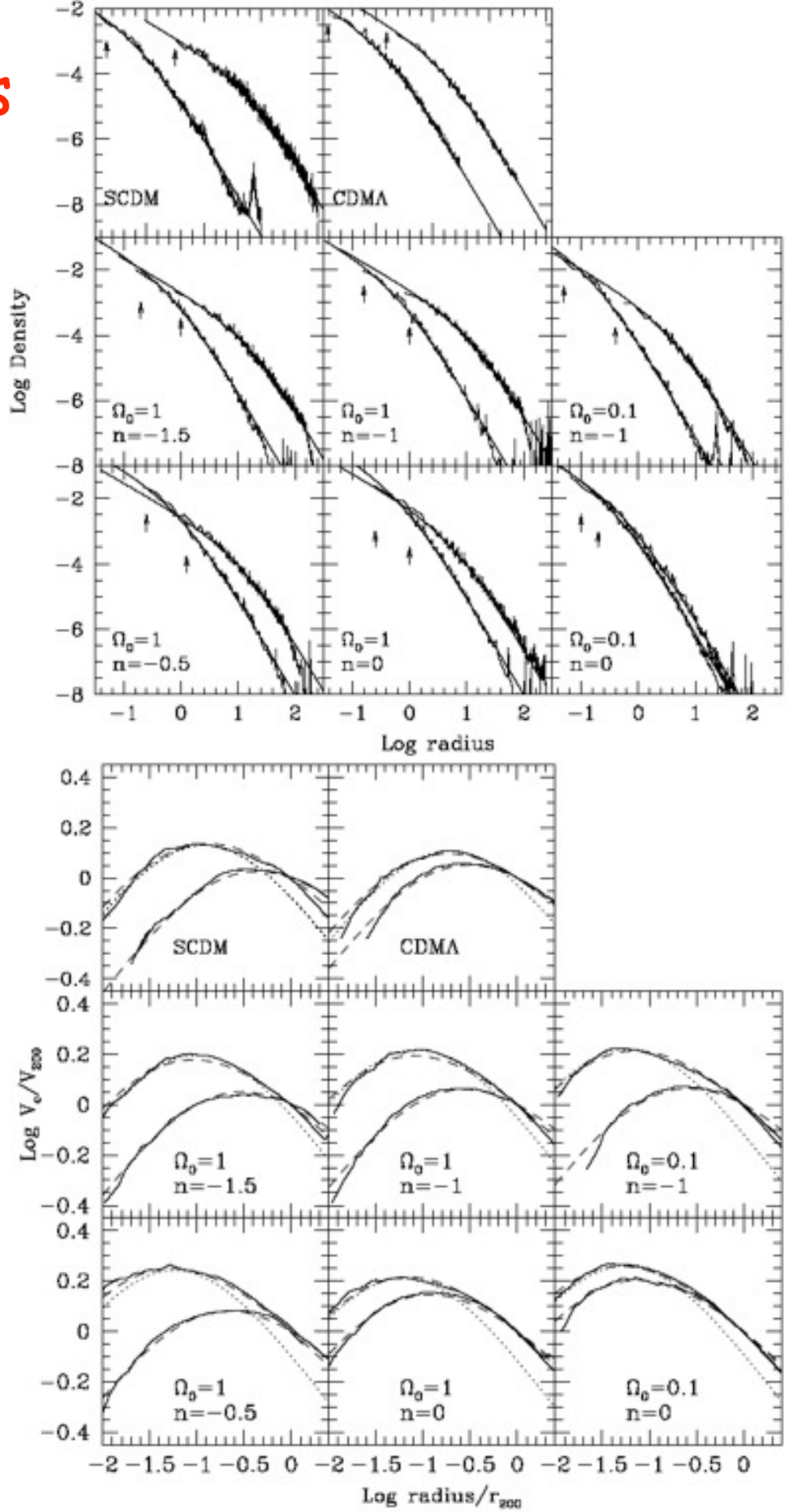

Dark Matter Halo Radial Profile

Comparison of NFW and Moore et al. profiles

Parameter	NFW	Moore et al.
Density $x = r/r_s$	$\rho = \frac{\rho_s}{x(1+x)^2}$ $\rho \propto x^{-3}$ for $x \gg 1$ $\rho \propto x^{-1}$ for $x \ll 1$ $\rho/\rho_s = 1/4$ at $x = 1$	$\rho = \frac{\rho_s}{x^{1.5}(1+x)^{1.5}}$ $\rho \propto x^{-3}$ for $x \gg 1$ $\rho \propto x^{-1.5}$ for $x \ll 1$ $\rho/\rho_s = 1/2$ at $x = 1$
Mass $M = 4\pi\rho_s r_s^3 f(x)$ $= M_{\rm vir} f(x)/f(C)$ $M_{\rm vir} = \frac{4\pi}{3}\rho_{\rm cr}\Omega_0\delta_{\rm top-hat} r_{\rm vir}^3$	$f(x) = \ln(1+x) - \frac{x}{1+x}$	$f(x) = \frac{2}{3}\ln(1+x^{3/2})$
Concentration $C = r_{\rm vir}/r_s$	$C_{\rm NFW} = 1.72 C_{\rm Moore}$ for halos with the same $M_{\rm vir}$ and $r_{\rm max}$ $C_{1/5} \approx \frac{C_{\rm NFW}}{0.86 f(C_{\rm NFW}) + 0.1363}$ error less than 3% for $C_{\rm NFW}$ =5-30 $C_{\gamma=-2} = C_{\rm NFW}$	$C_{\rm Moore} = C_{\rm NFW}/1.72$ $C_{1/5} = \frac{C_{\rm Moore}}{[(1+C_{\rm Moore}^{3/2})^{1/5} - 1]^{2/3}}$ $\approx \frac{C_{\rm Moore}}{[C_{\rm Moore}^{3/10} - 1]^{2/3}}$ $C_{\gamma=-2} = 2^{3/2} C_{\rm Moore}$ $\approx 2.83 C_{\rm Moore}$
Circular Velocity $v_{\rm circ}^2 = \frac{GM_{\rm vir}}{r_{\rm vir}}\frac{C}{x}\frac{f(x)}{f(C)}$ $= v_{\rm max}^2 \frac{x_{\rm max}}{x}\frac{f(x)}{f(x_{\rm max})}$ $v_{\rm vir}^2 = \frac{GM_{\rm vir}}{r_{\rm vir}}$	$x_{\rm max} \approx 2.15$ $v_{\rm max}^2 \approx 0.216 v_{\rm vir}^2 \frac{C}{f(C)}$ $\rho/\rho_s \approx 1/21.3$ at $x = 2.15$	$x_{\rm max} \approx 1.25$ $v_{\rm max}^2 \approx 0.466 v_{\rm vir}^2 \frac{C}{f(C)}$ $\rho/\rho_s \approx 1/3.35$ at $x = 1.25$

Klypin, Kravtsov, Bullock & Primack 2001

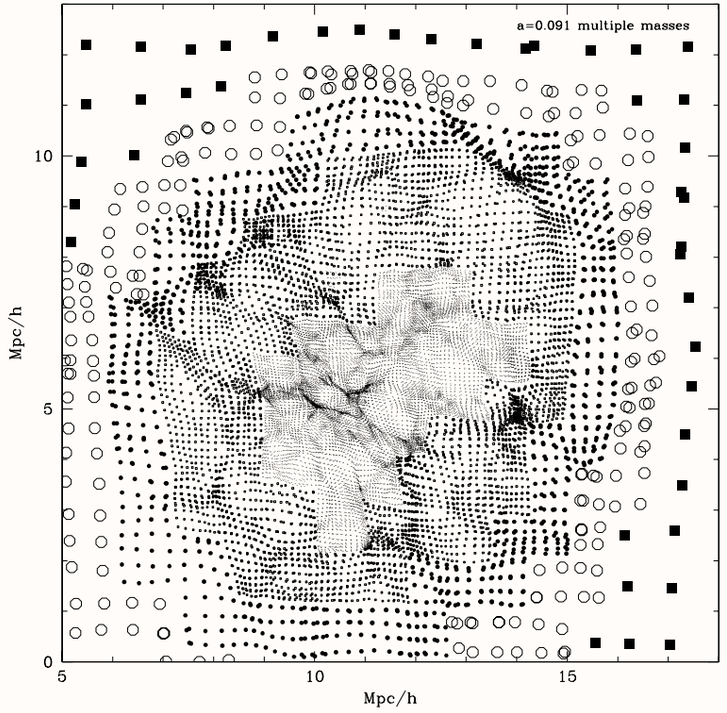

Fig. 2.— Distribution of particles of different masses in a thin slice through the center of halo A_1 (see Table 1) at $z = 10$ (top panel) and at $z = 0$ (bottom panel). To avoid crowding of points the thickness of the slice is made smaller in the center (about $30h^{-1}$kpc) and larger ($1h^{-1}$Mpc) in the outer parts of the forming halo. Particles of different mass are shown with different symbols: tiny dots, dots, large dots, squares, and open circles.

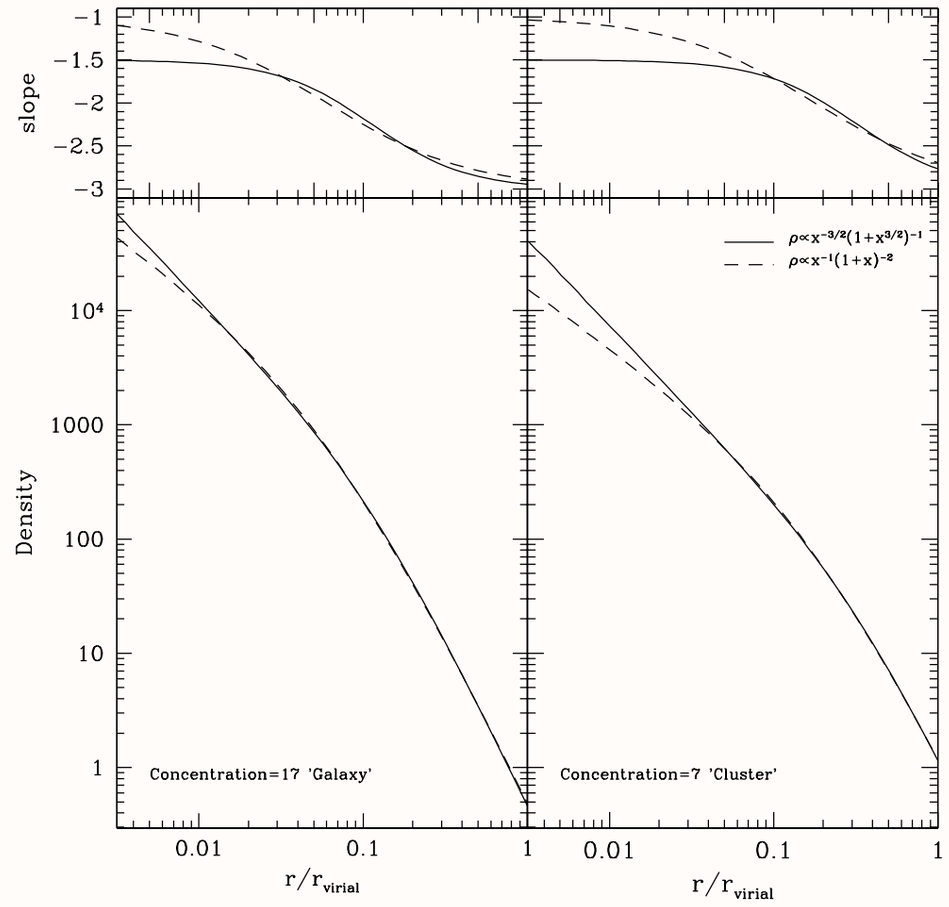

Fig. 3.— Comparison of the Moore et al. and the NFW profiles. Each profile is normalized to have the same virial mass and the same radius of the maximum circular velocity. *Left panels:* High-concentration halo typical of small galaxy-size halos $C_{\rm NFW} = 17$. *Right panels:* Low-concentration halo typical of cluster-size halos. The deviations are very small ($< 3\%$) for radii $r > r_s/2$. Top panels show the local logarithmic slope of the profiles. Note that for the high concentration halo the slope of the profile is significantly larger than the asymptotic value -1 even at very small radii $r \approx 0.01 r_{\rm vir}$.

Klypin, Kravtsov, Bullock & Primack 2001

Aquarius Simulation: Formation of a Milky-Way-size Dark Matter Halo

Diameter of Milky Way Dark Matter Halo
1.6 million light years

Diameter of visible Milky Way
30 kpc = 100,000 light years

Diameter of Milky Way Dark Matter Halo
1.6 million light years

500 kpc

Volker Springel
Max-Planck-Institute
for Astrophysics

Diameter of visible Milky Way
30 kpc = 100,000 light years

Diameter of Milky Way Dark Matter Halo
1.6 million light years

500 kpc

Volker Springel
Max-Planck-Institute
for Astrophysics